BNWL-1809
UC-70 2F

QUARTERLY PROGRESS REPORT
RESEARCH AND DEVELOPMENT ACTIVITIES
WASTE FIXATION PROGRAM
OCTOBER THROUGH DECEMBER 1973

Battelle
Pacific Northwest Laboratories
Richland, Washington 99352

JANUARY 1974

Prepared for the U.S. Atomic Energy
Commission under Contract AT(45-1):1830

BNWL-1809

NOTICE

The report was prepared as an account of work sponsored by the United States Government. Neither the United States nor the United States Atomic Energy Commission, nor any of their employees, nor any of their contractors, subcontractors, or their employees, makes any warranty, express or implied, or assumes any legal liability or responsibility for the accuracy, completeness or usefulness of any information, apparatus, product or process disclosed, or represents that its use would not infringe privately owned rights.

PACIFIC NORTHWEST LABORATORY
operated by
BATTELLE
for the
U.S. ATOMIC ENERGY COMMISSION
Under Contract AT(45-1)-1830

Printed in the United States of America
Available from
National Technical Information Service
U.S. Department of Commerce
5285 Port Royal Road
Springfield, Virginia 22151
Price: Printed Copy $5.45; Microfiche $1.45

AEC-RL RICHLAND, WASH.

3 3679 00062 1476

BNWL-1809
UC-70
Waste Disposal
and Processing

QUARTERLY PROGRESS REPORT
RESEARCH AND DEVELOPMENT ACTIVITIES
WASTE FIXATION PROGRAM
OCTOBER THROUGH DECEMBER 1973

Compiled by

A. M. Platt

Nuclear Waste Technology Department

January 1974

BATTELLE
PACIFIC NORTHWEST LABORATORIES
RICHLAND, WASHINGTON 99352

TABLE OF CONTENTS

LIST OF FIGURES v
LIST OF TABLES vii
INTRODUCTION 1
SUMMARY 1
COMMERCIAL WASTE FIXATION 2
SOLIDIFICATION EQUIPMENT - NONRADIOACTIVE DEVELOPMENT 2
Development Spray Calciner and Inconel Melter 2
Wiped Film Evaporator 9
Fluidized Bed Calciner 12
Ceramic Electrode Heated Melter 15
Ceramic Materials Molten Glass Compatibility 16
Cost of Improved Heat Transfer in Radioactive Waste Canisters 20
PRODUCT CHARACTERIZATION 25
Melt Development - Effect of Glass Composition on Leachability 25
Characterization of Crystallites in PW-4b Melts 34
Waste Vaporization Studies 42
Helium Generated Stresses and Bubbles in Waste Glass 51
Interim Storage of WSEP Radioactive Waste Canisters 56
Composition of Gas Inside WSEP Canisters 56
ALTERNATIVE WASTE FIXATION SCHEMES 58
Coating of Waste Calcine 58
Advanced Product Forms Research 62
Redundant Protection of Radioactive Wastes (The Russian Doll) 62
Isolation of Radioactive Wastes in Ceramic Matrices by Hot Pressing 63
High Density Hot Pressed Cement Materials in Radioactive Waste Management 64
Crystalline Phase Formation in Calcined PW-6 and PW-4b 65
Hot Pressing of PW-6/Quartz Mixtures 67
Hot Pressing of Cement and Cement: PW-6 Mixtures 68

Safety Analysis 69
AEC WASTE FIXATION 72
Ceramic Materials-Molten AEC Waste Compatability 72
DISTRIBUTION D-1

LIST OF FIGURES

1. PW-6 Waste Volume Reduction in the Wiped Film Evaporator . . 10
2. Wiped Film Evaporator Heat Transfer Coefficients with PW-6 Waste 10
3. Schematic Equipment Flowsheet for the Fluidized Bed Calciner 12
4. Schematic View of Electrode-Type Ceramic Melter 15
5. Cost of Finned Canisters 22
6. Annular Canisters - Constant Radius Versus Constant Volumetric Heat Generation Rate 23
7. Annular Containers - Cost Per Kilowatt for Constant Radius and Constant Heat Generation Rate 24
8. Comparison of Cost of Finned Canisters with Plain Canisters at Constant Volumetric Heat Generation Rate and Constant Canister Radius 26
9. Leachability of System SiO_2-B_2O_3-Al_2O_3-30 wt% PW-6 Calcine 32
10. Leachability of System SiO_2-B_2O_3-Al_2O_3-30 wt% PW-6 Calcine 33
11. Leachability of System SiO_2-ZnO - 11.5 wt% B_2O_3 - 2.5 wt% MgO - 1.5 wt% CaO - 30 wt% PW-6 Calcine 35
12. Leachability of the System SiO_2-B_2O_3-Na_2O-CaO-MgO - 45 wt% PW-4c Calcine 36
13. 100X Photomicrograph of "Second" Phase Area in PW-4b Type Glass 38
14. 1000X Scanning Electron Micrograph of "Second" Phase Area in PW-4b Type Glass 38
15. 4000X Scanning Electron Micrograph of Outlined Area in Figure 14 38
16. 20,000X Scanning Electron Micrograph of Matrix Area of the "Second" Phase from PW-4b Type Glass 39
17. 100X Photomicrograph of Glass Sample from Melter Run DSS-8 39
18. Volatilization Weight Loss from PW-4b Calcine 42
19. Volatilization Weight Loss of PW-4b Calcine Samples of Different Thickness at 1200°C 43
20. Volatilization Weight Loss from Composition 72-68 Borosilicate Glass 45

LIST OF FIGURES (contd)

21. Volatilization Weight Loss from Composition 72-68 Samples of Different Thickness at 1200°C 46

22. Volatilization Weight Loss Rate Versus Sample Thickness. . . 47

23. 8X Photomicrograph of a Sample of Glass from the DSS-8 Melter Run 49

24. Effect of the Volumetric Porosity of Solidified High-Level Waste on the Maximum Tensile Stress Induced 51

25. As Coated, Fluidized Bed, Waste Particles 57

26. Microstructure of Waste Particles Coated with Pyrolytic Carbon 58

27. Pyrolytic and Silicon Carbide Coated Waste Particles . . . 59

28. 100-Year Reference Waste Management System 69

29. Data for Volatilization from Solidified High Level Waste 71

LIST OF TABLES

1. Operating Parameters and Results of Development Spray Solidification Runs DSS-6 Through DSS-9 3
2. Expected Material Balance Conditions for the Fluidized Bed Calciner 13
3. Cost Comparison of Annular Canisters With Plain Canisters 27
4. Cost Comparison of Internally Finned Canisters With Plain Canisters 28
5. Cost Comparison for Fixed Volumetric Heat Generation Rate of Stainless Steel Pots With and Without Fins 29
6. Canister Cost in Dollars per Square Foot of Material . . . 30
7. X-ray Fluorescent Analysis of Vapor Deposits from a 0.64 cm Thick Sample of PW-4b Heated at 1200°C 44
8. Composition of Gas Phase Samples from WSEP Canisters
9. Atomic Concentrations in Wastes After Initial Drying . . . 64
10. 3 SiO_2: 1 PW-6 Hot Pressing Runs 65
11. Hot Pressing of Cements 67
12. Constituents of High-Level Liquid Wastes 72

QUARTERLY PROGRESS REPORT

RESEARCH AND DEVELOPMENT ACTIVITIES
WASTE FIXATION PROGRAM

OCTOBER THROUGH DECEMBER 1973

INTRODUCTION

This progress report is the fifth in a series that presents research and development activities in the field of radioactive waste fixation. Previous progress reports were BNWL-1699, 1741, 1761, and 1788.

SUMMARY

Two, 40-hr nonradioactive spray solidification runs were completed in which both PW-4b and PW-6 reference waste compositions were successfully converted into borosilicate glass. The throughput capacity of the 13-in. diameter spray calciner while processing PW-4b waste is over 38 ℓ/hr with a 700°C calciner wall and 24-30 ℓ/hr with a 550°C wall. Mechanical agitation increases the capacity of the inconel melter to over 4.5 ℓ of melt per hour and greatly improves product homogeneity.

Both PW-4b and PW-6 reference waste compositions were successfully concentrated in the nonradioactive, wiped film evaporator (WFE) facility. Either waste can be concentrated to approximately 60 wt% total solids in the WFE. For the PW-6 waste, this represents removal of about 80% of the initial liquid present in the waste.

Two ceramic melters were built and operated, each using molybdenum electrodes for heating. While the performance of these first melters indicated a number of design and construction problems which need to be resolved, a ceramic-electrode heated melter appears to be a viable alternative to metallic melters.

The PW-4b melt composition 72-68 contains finely divided crystallites when large quantities are melted at 1150°C. The crystallites were identified

as CeO_2, a spinel and zircon, with CeO_2 the predominant species. Several options for eliminating the crystallites include increasing the melt temperature, agitating the melt to prevent crystal settling, modification of the composition to promote CeO_2 solubility, and reducing the concentration of CeO_2 in the glass.

Helium gas formed by alpha particle emission from actinide nuclides in high-level waste glasses can produce large internal stresses in the glass. A porosity of 0.2% in typical waste glasses, from uranium oxide fuel, may be sufficient to reduce the internal stresses to inconsequential levels by providing sites for gas accumulation. However, for waste glasses from plutonium recycle fuel, a higher than anticipated porosity of approximately 3% may be required.

Mass spectrographic analysis was performed on the gas phase from several canisters of solidified radioactive waste from the previous Waste Solidification Engineering Prototypes (WSEP) program. Analysis of the gas in several phosphate glass canisters revealed CO_2, present from the decomposition of residual Purex solvent and silicone antifoam agent, and N_2O from the decomposition of nitrate. Hydrogen was below detection limits. Oxygen depletion of the original air atmosphere was the only change found in limited sampling of spray solidified and pot calcine product canisters.

COMMERCIAL WASTE FIXATION

SOLIDIFICATION EQUIPMENT - NONRADIOACTIVE DEVELOPMENT

Development Spray Calciner and Inconel Melter - W. F. Bonner, A. K. Postma

Four spray solidification runs numbered DSS-6 through DSS-9 were completed. (See Table 1) Run DSS-6 was a 41-hr run in which the high sodium PW-6 reference waste composition was solidified. Melt agitation, filter differential pressure and quench scrubbing of the off-gas were major considerations. DSS-7 was similar to DSS-6 except PW-4b feed was used and the usual condenser and scrubber were used for off-gas treatment.

TABLE 1. Operating Parameters and Results of Development Spray Solidification Runs DSS-6 through DSS-9

RUN NUMBER	DSS-6	DSS-7	DSS-8	DSS-9
DATE	9/12-14/73	10/9-11/73	11/2/73	11/12/73
FEED				
TYPE	PW-6	PW-4b	PW-4 b	PW-4 b
SPECIFIC GRAVITY	1.38	1.17	1.155	1.16
TEMPERATURE, ^{o}C	52	37	48	36
NOZZLE PRESSURE, psig	22	24	(c)	(c)
FEED RATE, ℓ/hr	9.6	16.0	(c)	(c)
TOTAL FEED CONSUMED, ℓ	393	637	451	120
NUMBER OF INTERRUPTIONS	2(b)	0	1(h)	0
TOTAL DOWN TIME, min.	238(b)	0	60(h)	0
ATOMIZING FEED NOZZLE (a)				
ATOMIZING AIR FLOW, scfm	5.4	5.5	(c)	(c)
ATOMIZING AIR PRESSURE, psig	40	40	(c)	(c)
ATOMIZING AIR TEMPERATURE, ^{o}C	55	51	(c)	(c)
CALCINER				
FURNACE TEMPERATURE, ^{o}C - ZONE 1	745	785	(c)	(c)
- ZONE 2	730	720	(c)	(c)
INTERNAL WALL TEMPERATURES, ^{o}C				
24 cm BELOW FEED NOZZLE	707	740	(c)	(c)
61 cm BELOW FEED NOZZLE (g)	700	700	700	550
99 cm BELOW FEED NOZZLE	705	690	(c)	(c)
147 cm BELOW FEED NOZZEL (g)	700	700	700	550
175 cm BELOW FEED NOZZLE	630	425	(c)	(c)
POWER CONSUMPTION, kW - ZONE 1	11.4	22.0	(c)	(c)
- ZONE 2	12.3	12.1	(c)	(c)
VACUUM, INCHES OF WATER				
NORMAL	10	10	6	10
DURING BLOWBACK	5.5	2	1	2
AIR INLEAKAGE, scfm	1.6	4.5	<1	<1
CALCINE				
MOISTURE CONTENT, %	1.66	0.66	0.91	NA
NITRATE CONTENT, %	34.7	0.61	0.15	NA
CALCINER VIBRATOR				
CYCLE TIME, min.	1	2	5	5
PULSE TIME, sec.	2	2	1	1
AIR SUPPLY PRESSURE, psig	60	60	40	40

RUN NUMBER	DSS-6	DSS-7	DSS-8	DSS-9
CALCINER OFFGAS FILTERS				
BLOWBACK AIR TEMPERATURE, °C	400	400	350	400
BLOWBACK AIR PRESSURE, psig	30	100	100	60
BLOWBACK CYCLE, min.	2	2	5	5
BLOWBACK PULSE, sec.	1	1	1/4	1/4
FILTER PRESSURE DROP, in. OF WATER				
- START	2.5	1.5	---	---
- END	3.7	10	20 (i)	12.5 (j)
TOTAL NONCONDENSIBLE FLOW TO FILTERS, scfm	8.9	10	12 (i)	9 (j)
TOTAL GAS FLOW TO FILTERS, acfm	37.2	33	82 (i)	64 (j)
FILTER CHAMBER TEMPERATURE, °C	400	425	(c)	(c)
FILTER FACE VELOCITY, ft./min.	2.40	2.2	5.3 (i)	4.14 (j)
PERMEABILITY, ft/min-in OF WATER				
- START	0.96	1.4	---	---
- END	0.64	0.22	0.28 (i)	0.33 (j)
SOLIDS DE-ENTRAINMENT FACTOR (d)	1000-4900	140-320	150-300	NA
MELTER				
FURNACE TEMPERATURE, °C	1165	1175	(c)	NOT USED
INTERNAL MELT TEMPERATURE, °C	1100	1140	(c)	
FREEZE VALVE TEMPERATURE, °C				
WHILE FROZEN	680	550	600	
AT START OF DRAINING	850	820	950	
WHILE DRAINING	825	1000	1125	
AT END OF DRAINING	650	900	650	
MELT PRODUCTION RATE, ℓ/hr	2.1	1.6	(c)	
MELT VISCOSITY, POISE (e)	110	209	NA	
MAXIMUM MELT DISCHARGE RATE, ℓ/min	0.71	1.5	NA	
RESIDENCE TIME, hr	1.6	1.4	(c)	
FURNACE POWER, kW	13.4	12.5	(c)	
PRODUCT				
WEIGHT, kg	272	209	61.3 (k)	9.6
VOLUME, ℓ	93.1	64.4	19.2	6.4
DENSITY, g/cc	2.92 (c)	3.24	3.20	1.5
FEED-TO-PRODUCT VOLUME RATIO	4.58	9.9	9.4	18.7
EQUIVALENT WASTE, TONNE	1.05	1.7	0.48 (k)	0.32
CALCINE CONTENT OF PRODUCT, %	25.7	23.0	23.7	100
SOLIDS ADDITION				
ADDITIVE (f)	FRIT 73-1	FRIT 73-1	FRIT 73-1	NONE
FRIT SIZE, mesh	6 TO 20	6 TO 20	6 TO 20	
BATCH SIZE, g	75	28.6	28.9	
ADDITION RATE, kg/hr	4.9	4.04	(c)	
TOTAL ADDED, kg	202	161	46.7	
FEEDER TYPE	SCREW FEEDER AND AIR LOCK	SLIDE VALVE AND AIR LOCK	SLIDE VALVE AND AIR LOCK	

RUN NUMBER	DSS-6	DSS-7	DSS-8	DSS-9
CONDENSER				
BOTTOMS M HNO_3 - START	(ℓ)	-0-	0.0	0.0
- END		0.81	0.9	NA
ACCUMULATION RATE, ℓ/hr		14.9	(c)	(c)
TOTAL ACCUMULATION, ℓ		598	398	124
SCRUBBER				
CIRCULATION RATE, ℓ/min	5-20	10	10	10
BOTTOM, M NaOH - START	6.3	8.64	6.8	NA
- END	NA	4.29	4.2	NA
ACCUMULATION RATE, ℓ/hr	9.6	1.4	(c)	0
TOTAL ACCUMULATION, ℓ	NA	56	8	0

NA - NOT AVAILABLE

(a) - EXTERNAL MIX PNEUMATIC ATOMIZING NOZZLE - SPRAYING SYSTEMS CO., SETUP #42

(b) - FEED INTERRUPTIONS CAUSED BY A LEAK IN THE NOZZLE CLEANOUT NEEDLE PACKING AND SEAL LEAKAGE IN THE CAUSTIC PUMP CAUSED A LOSS OF CAUSTIC.

(c) - VARIED DURING THE RUN.

(d) - BASED ON ANALYSES OF Cr, AND Ni

(e) - CALCULATED FROM THE HAGEN-POISEVILLE LAW

(f) - COMPOSITION REPORTED IN APRIL 1973 QUARTERLY PROGRESS REPORT, PAGE 3

(g) - USED TO CONTROL CALCINER FURNACE OUTPUT

(h) - SHUT DOWN TO REMOVE MELTER

(i) - AT TIME GAS FLOW THROUGH SEAL POT BEGAN DURING CAPACITY TEST

(j) - AT 39.6 ℓ/hr CALCIUM FEEDRATE DURING CAPACITY TEST

(k) - ONLY 180ℓ OF FEED WERE INCORPORATED INTO GLASS

(ℓ) - QUENCH SCRUBBER ONLY

Runs DSS-8 and DSS-9 investigated the capacity of the spray calciner operating with wall temperatures of 700 and 550°C, respectively. Melter capacity with mechanical agitation was also studied.

Calciner

Following 41 hr of PW-6 solidification, a 1-2 mm deposit was observed covering the top half of the calciner. As indicated by calciner furnace and wall temperatures, the scale reached steady state during the first hour of operation and did not change throughout the run.

A uniform wall scale about 0.5 mm thick was observed following 40 hr of processing PW-4b waste. The film had no observable effect on calciner performance.

Apparently, most of the calcination of PW-4b feed occurs in the upper half of the calciner. With a constant wall temperature of 700°C, the upper half of the calciner consumed 22 kW compared with 12 kW for the lower half.

Runs DSS-8 and DSS-9 investigated the calciner capacity for processing PW-4b waste. During these runs the calciner feed rate was increased hourly by about 3 ℓ/hr until wall scaling was evident. At a wall temperature of 700°C the liquid flow rate at which scaling occurs in the 13-in. calciner is 38-45 ℓ/hr, and at 550°C the scaling flow rate is 24-30 ℓ/hr.

A calcine production run, DSS-8A, was made at the same operating conditions as DSS-8 except the PW-4b feed was concentrated to 60% of the original volume prior to the run. The run was prematurely terminated at a liquid feed rate of 35 ℓ/hr before scaling became apparent. From this data it appears that feed concentration has little effect on calciner capacity and that economics in calciner equipment can be realized by pre-evaporating the calciner feed.

During DSS-7 in which PW-4b waste was solidified, the filter differential pressure (DP) was observed to reach a maximum. In the first 20 hr of operation at a filter face velocity of 2.2 ft/min, the off-gas filter DP increased to 10 in. of water then remained at that level for the remaining 20 hr of the run. Changing filter blowback conditions during the run had little effect on filter DP but apparently, 1/4 sec pulses of 100 psig air

at 5 min intervals are as effective as longer more rapid pulses. A short pulse also reduces calciner pressurization during blowback.

Melter

During DSS-8 a melter capacity of 4.6 ℓ/hr of melt was obtained by mechanically agitating the melt. This is more than twice the capacity of the melter without an agitator.

Without agitation the high viscosity (100-250 poise) of the melt limits melter capacity because 1) incoming calcine and frit cannot readily mix with the melt, and 2) convective heat transfer is severely limited. These conditions combine to produce melt temperatures in the lower part of the melter which approach furnace temperature while the melt-calcine surface is as much as 500°C cooler. With agitation the melt temperature is uniform and melter capacity is limited by the rate of heat transfer to the melter crucible.

Greatly improved product homogeneity is a second benefit of melt agitation. Without melter agitation heavy insoluble crystallites mainly CeO_2, tend to settle out and, with time, even restrict the 1/2-in. melt discharge tube. Agitation effectively disperses the crystallites facilitating melter draining. Draining the melter while calcine and frit were being added to it did not adversely effect product homogeneity.

Agitation by both mechanical mixing and sparging was investigated. Sparging with 30 scfh of argon increased the melter capacity by 50% but introduced splashing problems and would undoubtedly increase Ru evolution from the melter. After careful evaluation it was concluded that use of the more complex mechanical agitator is justified due to its higher agitation efficiency and potential volatiles retention capability compared to sparging.

The PW-6 melt formulation used during DSS-6 was very corrosive. Severe pitting as much as 3-mm deep occurred in the Inconel 690 melter after 48 hr of contact with the PW-6 melt. The melt composition is therefore being changed and new melt formulations are presently being developed which will reduce the corrosion to acceptable levels.

Product

Three, 20-cm diameter cans were filled with borosilicate glass produced from both PW-4b and PW-6 feeds. Can conditions during filling were 1) no external heating, 2) no external heating during filling followed by heating to 900°C then cooling at 25°C/hr and 3) product receiving furnace maintained at 425°C during can filling followed by cooling at 25°C/hr.

Product from cooling condition 1 shattered during cooling into 1 to 2 in. size pieces, while glass cooled per conditions 2 and 3 remained in considerably larger pieces. The surface of these pieces, however, was covered with a thin layer of fine dust which increases the surface available for leaching.

Thermocouples in the product showed that internal temperatures remain at over 700°C for as long as 2 hr during cooling. At these temperatures microscopic crystals formed producing a gray product in the interior of the can. The product had a shiny black surface where it cooled more rapidly.

Inclusions in the product differed, depending on melt composition and agitation. Product from PW-6 feed contained many, approximately 1-mm diameter, inclusions of bright yellow $NaMoO_3$, but was otherwise homogenious. Product from PW-4b melt dumped without melter agitation contained collections of CeO_2 crystallites up to 2-cm in diameter and sharp product composition changes at the melter dump interfaces. Glass produced from PW-4b feed that was agitated while in the melter contained inclusions which were < 1-mm in diameter and widely separated. Pinpoint voids were observed throughout all of the borosilicate product.

Off-Gas Decontamination

Quench scrubbing was proposed as a method for reduction of radioactive ruthenium in the calciner off-gas. During run DSS-6, hot off-gas from the filters was routed directly to a 14-in. diameter scrubber filled with 1-in. raschig rings. In the scrubber, upflowing off-gas was quenched and scrubbed with cooled 6 M NaOH. Mass transfer proceeded normally and, as evidenced by readings from thermocouples placed in the packed column, all heat transfer was accomplished in the lower few inches of packing.

Decomposition products of the various nitrate compounds in the feed were observed to react with and neutralize the caustic. About 2 moles of NaOH caustic were neutralized per mole of HNO_3 in the feed.

Wiped Film Evaporator - R. D. Dierks, A. K. Postma

Both PW-4b and PW-6 simulated waste compositions were successfully concentrated in the nonradioactive, wiped film evaporator test facility. Eight runs, using simulated waste compositions as feed, were completed to evaluate the characteristics of the test unit. The first two runs utilized a PW-4b feed and explored quickly the operating variables of rotor speed, paddle clearance, jacket steam pressure, and feed flow rate. The last six runs utilized a PW-6 feed and the operating variables were limited to the jacket steam pressure and the feed flow rate. With a 450-rpm rotor speed, and a 1/32-in. paddle clearance, the highest total solids concentration that could be achieved in the concentrate, with either feed material, was about 60 wt% total solids. With the PW-4b composition, and 120 psig steam on the jacket, the feed rate to the evaporator was limited to about 30 ℓ/hr to realize this maximum concentrate composition. However, with the PW-6 composition, 60 ℓ/hr of feed were evaporated to this same maximum total solids content, with only 80 psig steam in the jacket.

Prior to the last three runs, WFE-6, 7 and 8, a heat exchanger and a temperature control system were added to the feed system to enable the temperature of the feed entering the evaporator to be controlled at a value about 1°C (±0.5°C) below its boiling point. This eliminated another operating variable and simplified the calculation of heat transfer coefficients.

The performance of the unit in evaporating the simulated PW-6 waste is shown in Figures 1 and 2. Figure 1 shows the relationship between the jacket steam pressure (or temperature) and the fraction (in percent) of the liquid portion of the feed that was evaporated, at various feed rates. These curves indicate that about 80% of the initial liquid present in a PW-6 waste can be removed in this evaporator, regardless of the feed rate, when it is operated at 450 rpm with a 1/32-in. clearance between the paddle and the evaporator barrel. Physically, this maximum is characterized by a dense caking of solids on the evaporator barrel and a subsequent overloading of the rotor drive unit

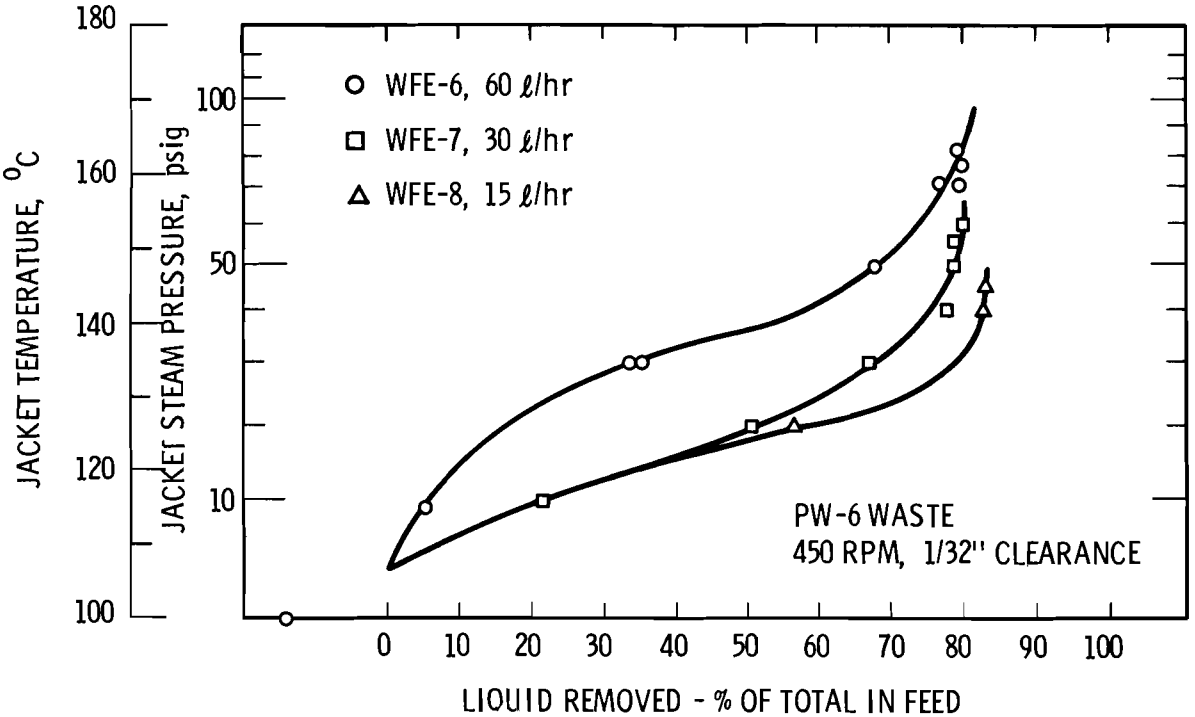

FIGURE 1. PW-6 Waste Volume Reduction in the Wiped Film Evaporator

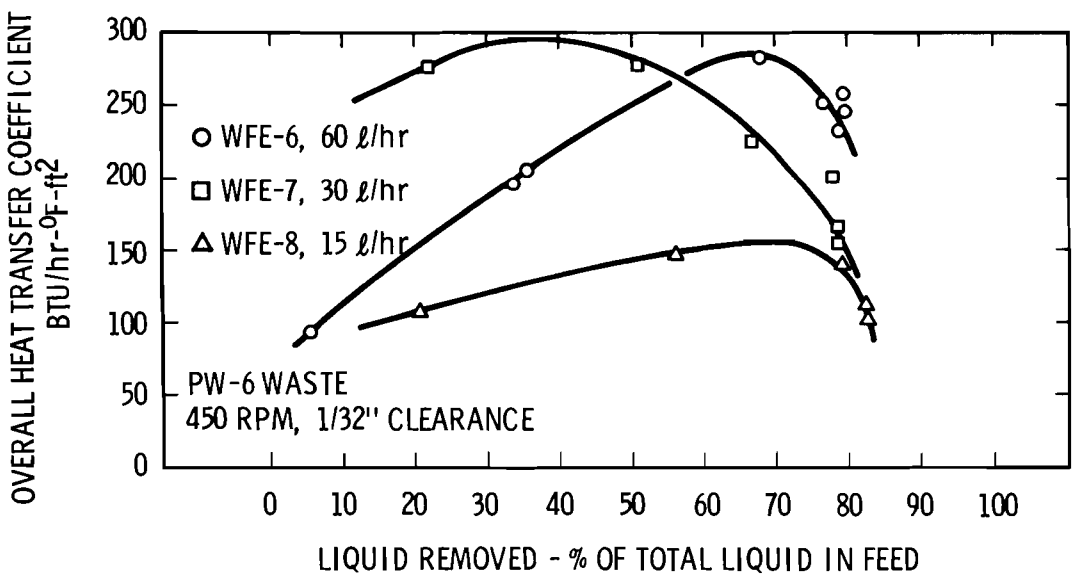

FIGURE 2. Wiped Film Evaporator Heat Transfer Coefficients with PW-6 Waste

as the paddles scrape the top off of the tightly adhering cake. At lower volume reduction values, about 70% liquid removal or less, the barrel walls remain free of incrustations. A 70-80% reduction in the liquid content of PW-6 at a feed rate of 100 ℓ/hr appears to be feasible with this unit operating at the maximum available pressure of 120 psig.

The heat transfer characteristics of the unit, for the operating conditions of these later experiments, are presented in Figure 2, and show quite clearly the decrease in the heat transfer coefficient in the region where the heat transfer surface is beginning to become covered with the dense, nonconducting scale.

Additional experiments are planned to clarify the variable effect of feed rate on the heat transfer coefficient values and to clarify the low and erratic heat transfer coefficients observed at low evaporation rates.

Fluidized Bed Calciner - W. J. Bjorklund, D. H. Siemens

The design work for a fluidized bed calciner, to be installed in 324 Building engineering laboratory is completed and fabrication is to begin at the end of the period. The unit is a prototype for a calciner to be installed in the hot cell. A majority of the design criteria for this equipment was provided by Allied Chemical Corporation, Idaho Falls, Idaho. The detailed equipment design was completed at Pacific Northwest Laboratories.

The unit is designed for the processing of PW-4b waste at a rate of 15 ℓ/hr at 500°C. Process heat will be supplied by the in-bed combustion of oxygen and kerosene. Fixation of the solid waste product in borosilicate glass will be done by connecting the calciner unit to an existing melter and melt receiver.

The calcining vessel is a 6.75-in.-square spool piece with a 9-in.-square disengaging section. A 12-in.-diameter filter chamber, containing seven 36-in.-long by 2 3/4-in.-diameter sintered metal filters is used to remove entrained fines from the process off-gas. The filters are blown back periodically by a pulse of high pressure air. The filtered off-gas then passes through an existing condenser and scrubber system for clean-up. A flowsheet and material balance for the system are shown on Figure 3 and Table 2.

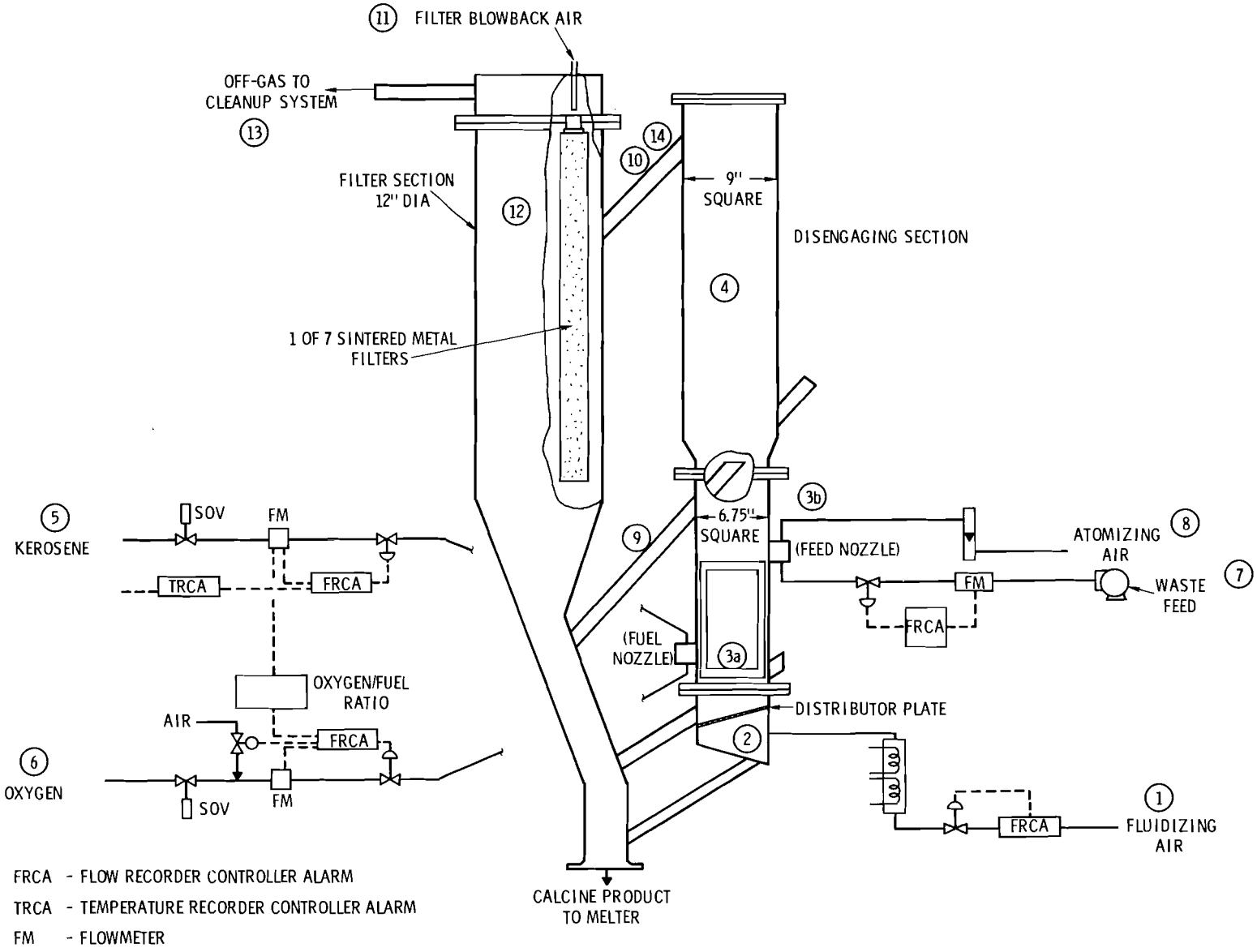

FIGURE 3. Schematic Equipment Flowsheet for the Fluidized Bed Calciner (Note: Stream Numbers Are Keyed to Flows in Table 2)

TABLE 2. Expected Material Balance Conditions for the Fluidized Bed Calciner

	1 FLUIDIZING AIR	2 PLENUM	3a BED (BELOW NOZZLES)	3b BED (ABOVE NOZZLES)	4 DISENGAGING SPACE	5 FUEL	6 FUEL ATOMIZING OXYGEN	7 WASTE FEED	8 FEED ATOMIZING GAS	9 PRODUCT	10 CALCINER OFF-GAS	11 FILTER BLOWBACK AIR	12 FILTER VESSEL	13 FILTERED OFF-GAS	14 FINES
TEMPERATURE - ^{0}C	20	400	500	500	450	20	15		20	<500		<150	>350	>250	
PRESSURE - psig	50	2.0				80	80	<5.0	50			<100			
VACUUM - "H_2O		* *		*	10								12	20	
LIQUID RATE - l/hr						3.0		15.0							
GAS RATE - scfm-(acfm)	<8.0		(<20)	(<42)	(<40)		<4.0		<4.0				(<34)		
VELOCITY - ft/sec			<1.0	<2.2	<2.8 (WET)						<100 (WET)		<0.07		
SOLIDS RATE - gm/hr										800					400
SOLIDS LOADING - gr/acfm											<0.10				
NOZZLE AIR RATIO						<2100		<450							

* ΔP ACROSS BED EXPECTED <30 "H_2O

* * ΔP ACROSS DISTRIBUTOR PLATE <20 "H_2O

The fluidized bed calciner will provide the opportunity to (1) solve the problems associated with coupling to a melter, (2) work out potential remotability problems associated with radioactive operation, (3) gain operating experience prior to radioactive "hot" cell use, and (4) allow additional experimenting with processing concepts to solve potential "hot" cell operating problems. Some of the alternative means of operation that may be considered are (1) new and more efficient means of product withdrawal, (2) use of an inert bed, (3) improved and alternative process heating methods, (4) recycling of off-gas, and (5) steam fluidization.

Ceramic Electrode Heated Melter - R. B. Daken, C. C. Chapman, and A. K. Postma

Two ceramic melters were built and operated during this quarter, each using molybdenum electrodes for heating.[a] A schematic view of the melters is shown in Figure 4. The results of test runs made with these melters provided significant information necessary for designing a reliable unit. While the performance of these first melters pointed up a number of design and construction problems which need to be resolved, a ceramic electrode heated melter is a viable alternative to metallic melters.

The melters were tested relative to their ability to melt both glass frit and a frit-calcine mixture (ratio 3:1). Important considerations identified to date and deemed necessary are:

- A safe, reliable startup technique suitable for remote starting
- An electrode material with high corrosion resistance
- A ceramic material with high corrosion resistance
- A means of eliminating unnecessary metal constituents from the melter.

Each of the above problems is under investigation; the ceramic material problem is discussed elsewhere in this report. A second generation melter that will be coupled to a calciner or evaporator is currently being designed.

(a) Quarterly Progress Report, BNWL-1788, October 1973.

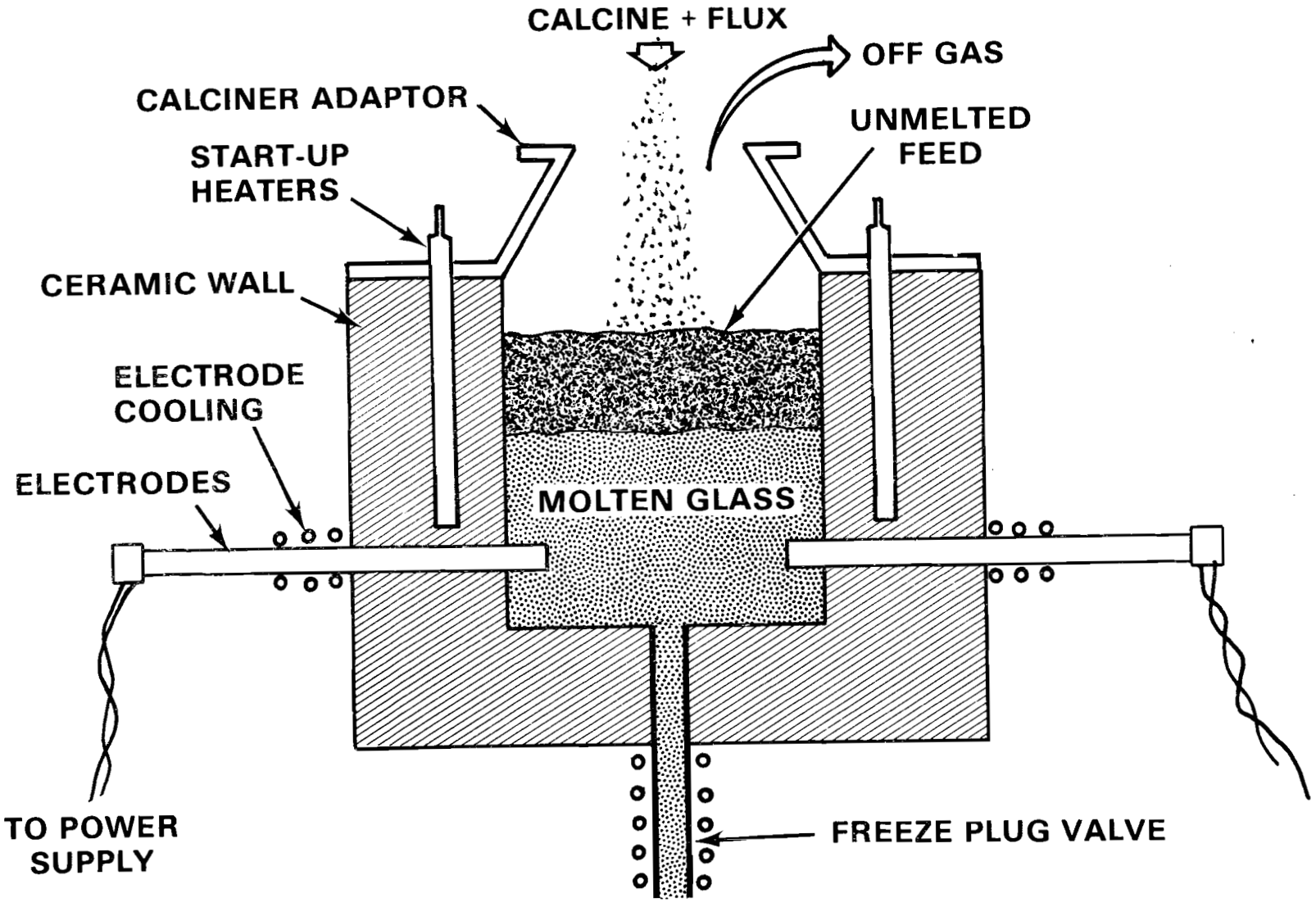

FIGURE 4. Schematic View of Electrode-Type Ceramic Melter

Ceramic Materials Molten Glass Compatibility - J. L. Bates

Ceramic refractories are being tested in a high temperature waste glass to determine the compatibility for use in a ceramic-lined waste glass melter. A number of refractory oxides and silicon carbide were tested. Initial results and a description of these tests were reported in the previous quarterly report.[a]

The waste glass was melted in air in a platinum crucible to 1450°C with the sample suspended in the hot zone of the furnace directly above the glass. Each sample was a parallelpiped approximately 0.4 in. square and 1 1/2 to 2 in. long. On reaching the desired temperature, the sample was lowered into the glass on a platinum wire. One half of the sample was immersed while the other half remained out of the liquid. Each sample was initially exposed for 48 hr in the molten glass, quickly removed within approximately 20 sec, and wrapped in a refractory wool to reduce thermal shock. The samples were then sectioned and examined ceramographically. Sibling samples of the compositions which exhibited the least amount of interaction with the molten glass were heated at 1450°C for 168 hr and examined.

The simulated waste glass (73-109) composition was composed of 51.1 wt% SiO_2, 12.5 wt% ZnO_2, 6.3 wt% ZrO_2, and 30 wt% PW-6 waste calcine. (The waste glass contained approximately 8.5 wt% Na_2O).

A number of commercial refractories were tested. These include:

168 hr at 1450°C

- Chrome (fused) - 79% Cr_2O_3
- Alumina-Chrome (fused) - 27% Cr_2O_3-60% Al_2O_3
- ZrO_2 - 95% zirconium oxide

(a) Quarterly Progress Report, BNWL-1788, pp. 7-9, October 1973.

48 hr at 1450°C

- ZAS (Sintered) - $Al_2O_3 \cdot ZrO_2 \cdot SiO_2$
- ZAS (fused) - $Al_2O_3 \cdot ZrO_2 \cdot SiO_2$
- SiO_2 (fused) - 96% SiO_2 with some Al_2O_3
- Zircon - Sintered $ZrO_2 \cdot SiO_2$
- SiC - SiC
- ZrO_2 (cast) - 95% ZrO_2 castable
- Chrome (isopressed) - 79.5% Cr_2O_3
- Chrome (fused cast) - 79.5% Cr_2O_3
- Alumina-Chrome (fused) - 60% Al_2O_3-27% Cr_2O_3
- Alumina (fused) - 95% Al_2O_3

Four of the refractories exhibited superior resistance to attack by molten waste glass i.e., Zircon, ZrO_2, fused and isopressed chrome ore and silicon carbide. The resistance of these refractories was significantly better than for any of the other refractories tested. One should note that the resistance of the fused cast chrome refractory was noticeably better than that for the isopressed refractory. The zircon, ZrO_2 and SiC exhibited slightly better resistance than the chrome ores, however, further evaluation is required.

The results indicate that the Al_2O_3 in the refractory reacted with the ZnO in the waste glass resulting in deterioration of the refractory surface. The data show:

- All refractories which contained Al_2O_3 in significant amounts appeared to react with the waste glass (73-109), with perhaps the exception of the fused, high density chrome ore. (The reason is not known.)
- Breakup of the surface resulted with limited penetration into the refractory.
- Oxide crystals were found in the glass adjacent to the refractory surface. There were both large crystals ($\sim$0.012 cm) and small ($\sim$0.0005 cm) partially crystalline particles.

An intensive electron scanning microscope and microprobe analysis was conducted on the 60% Al_2O_3-27% Cr_2O_3. These results demonstrated that:

- Crystals in the glass were basically $ZrO_2 \cdot SiO_2$ with little zinc, sodium, or aluminum present.
- The glass immediately adjacent to the refractory was depleted of zinc but higher in zirconium.
- The reaction area had a high concentration of zinc, aluminum, and chromium with minor amounts of iron.
- The refractory was two phase as it was originally.
- The matrix was high in aluminum and chromium and contained minor amounts of silicon and sodium. The lighter, but substantial second phase was higher in chromium and contained substantial aluminum but less than in the matrix. There were also moderate amounts of iron, zinc, and sodium.

The following mechanism of reaction between the refractories which contain Al_2O_3 and the (73-109) molten waste is suggested. The zinc in the glass and the Al_2O_3 in the refractory react forming $ZnO \cdot Al_2O_3$. [The reported phase diagram of ZnO and Al_2O_3 indicate a zinc aluminate composition in equal molar composition.] The zinc is removed from the waste adjacent to the reaction area. This depletion results in the crystallization of zircon crystals ($ZrO_2 \cdot SiO_2$) since it appears that the zinc is required to keep the ZrO_2 in solution.

A more complete description of the results for the better refractories is described below. The results for those which exhibited extensive reactions with the glass were similar to the results described in the previous quarterly report (BNWL-1788).

- ZAS (Sintered and fused) - Both the sintered and the fused cast alumina zirconia silicate reacted with the glass at the melt-refractory interface. Large crystals were found in the glass adjacent to the refractory surface.

- SiO_2 (fused) - The SiO_2 reacted only in selected areas near the surface. This reaction was not extensive but appeared as a change in microstructure which penetrated as spikes into the oxide. This oxide contained ∿1% Al_2O_3. Small crystals were found in the glass immediately adjacent to the surface.
- Zircon - The glass did not react with the zirconium silicate. The low density (26-38% porosity) allowed the liquid to penetrate the interconnecting pores but no reaction could be seen.
- Silicon Carbide - The silicon carbide, obtained from an unused, broken "glow-bar" heating element did not react with the glass. The molten glass penetrated the carbide slightly because of the small interconnecting porosity.

Results for three oxides subsequently tested for longer periods of 168 hr are:

- Fused Alumina-Chrome - The fused alumina-chrome was tested at longer periods in an attempt to define the reaction mechanism which appeared to relate to the presence of Al_2O_3 in the refractory.
- ZrO_2 - The 95% ZrO_2 cast refractory still exhibited unusual resistance to chemical attack by the waste glass. The molten glass penetrated the interconnecting pores of the low density ZrO_2. A thin reaction layer was observed on the outer surface of the oxide. This layer, 0.001-0.002 cm thick was dense and did not penetrate into the pores of the refractory. No reaction was observed beyond the rough surface of the ZrO_2.
- Fused Chrome - This high chrome, fused refractory showed only minor and perhaps questionable evidence of reaction with the waste glass. The glass did not penetrate into the oxide because of the high density and limited closed porosity. The microstructural examination indicated a slight possible change in the refractory at the surface. This was seen as a possible elimination of a second, lighter phase immediately at the surface, which was observed through the remainder of the refractory. There also appeared to be a slight, non-uniform breakup of the oxide at

the surface. Both of these effects were difficult to identify, since the reaction area had the identical-appearing structure as the matrix of the oxide.

Cost of Improved Heat Transfer in Radioactive Waste Canisters - G. Jansen and J. D. Kaser

In the analysis of heat transfer from radioactive waste canisters, there are two additive temperature differences to consider. The first is the temperature rise from the surroundings to the surface of the canister. This is highly dependent on the environment in which the canister is found and is often sufficient information if the surface temperature is the controlling design factor. If the design limitation is at the can centerline, the internal rise from the surface to the centerline must be added to the external rise to define design conditions. The relative importance of the two temperature rises varies with the external conditions. For direct burial in the soil the internal rise is secondary; in storage in water basins it is controlling.

The internal temperature rise and the effect on canister cost of attempts to reduce it were analyzed. Three assumptions are made in this treatment: (1) the thermal properties of the waste are temperature independent, (2) the temperature rise from canister surface to waste centerline is fixed, and (3) there are no heat losses due to end effects.

The initial phases of the study were reported in the final reports of the Waste Solidification Program.[a] A recent summary of further work was presented at the Winter 1973 ANS meeting.[b]

The first step in the study was to set up a matrix of variation. This matrix included plain cylindrical canisters, annular canisters, and cartridge-type internal fins with materials of construction being stainless steel and carbon steel. The canister length was 10 ft and the diameter

---

(a) WSEP Report, BNWL-1667, vol. 11, pp. 8.83-8.95, July 1972.

(b) G. Jansen and J. D. Kaser, "Improved Heat Transfer in Radioactive Waste Canisters," BNWL-SA-4753, November 1973.

ranged from 6 in. to 4 ft. Standard pipe sizes were used in all cases. Two inner-to-outer annulus ratios were used for the annular canisters, and 3, 5 and 7 fins were in the fin cartridges.

The second step involved obtaining cost estimates from vendors and architect engineers for each geometry presented for a fixed total volume of waste (usually 500 to 1000 canisters). Three vendors and one architect engineering firm made estimates. A typical cost estimate range is given in Figure 5 for finned canisters.

The final step in the analysis was to make cost comparisons of annular and finned canisters with plain canisters at fixed volumetric heat generation rate and at fixed total canister radius.

A cost comparison could imply a fixed radius when changing from a plain cylindrical canister to one with improved heat transfer. In reality as shown in Figure 6 for annular canisters there is no such limitation. In the upper figure the heat generation rate ratio is given as a function of the inner-to-outer-radius ratio. The comparison with plain cylinders might be made in either of two ways. In Situation I (middle left) the waste fixation process is unaltered so that the volumetric heat generation rate is fixed and the radius of the annular canister must be increased to take advantage of the increased allowable heat generation per canister. In Situation II (middle right) the canister radius is fixed and the waste fixation process is modified to increase the volumetric heat generation rate for the annular canister. Clearly, the annular canisters of Situation II are cheaper but processing costs may be higher. Shipping costs may be either higher or lower depending on tradeoffs between costs of physical handling, shielding and heat removal. The contrast between the two situations is most apparent when comparing the surface heat fluxes as shown in the lower figure (Figure 6). In Situation II the heat flux ratio increases without limit as the central hole gets bigger and slab behavior is approached, while in Situation I the heat flux ratio approaches $\sqrt{2}$ as slab behavior is approached for the annulus.

In Figure 7 are given actual cost comparisons for annular canisters based on estimates supplied by architect engineers and vendors. These are for quantities of 100 to 1000 canisters, 10 ft long, for use with calcined

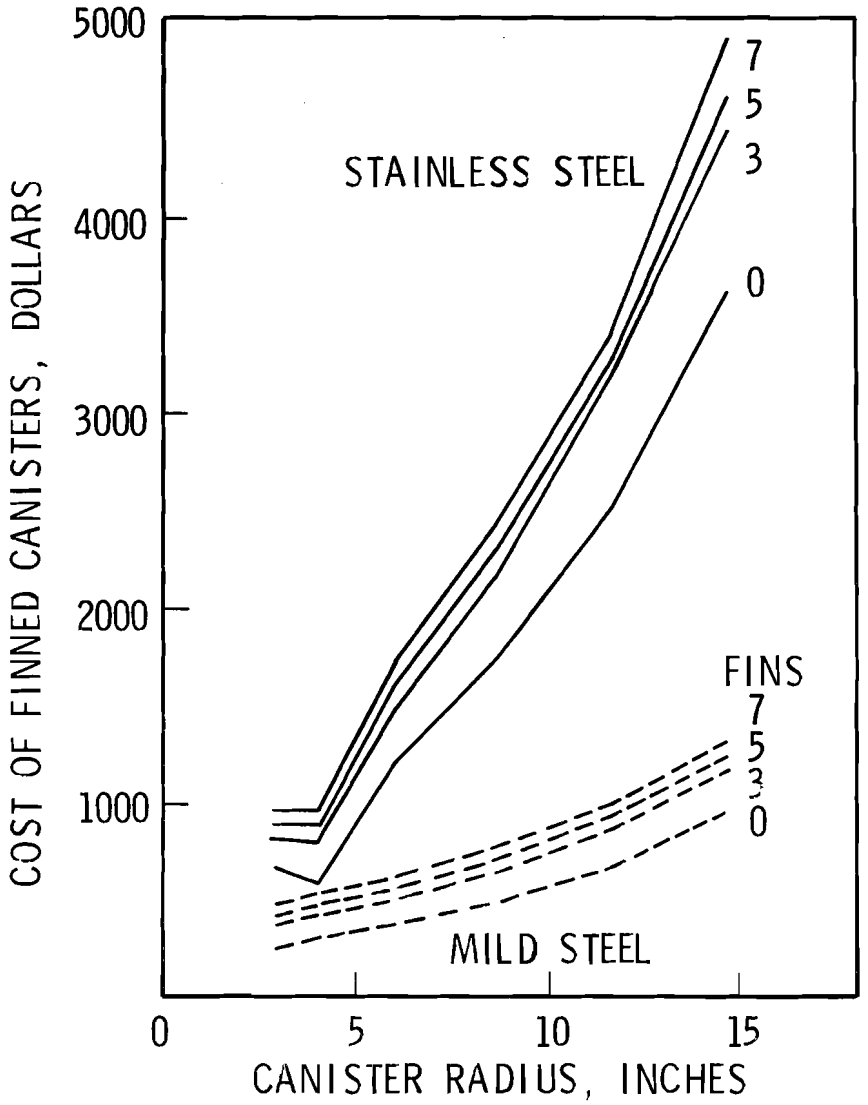

FIGURE 5. Cost of Finned Canisters

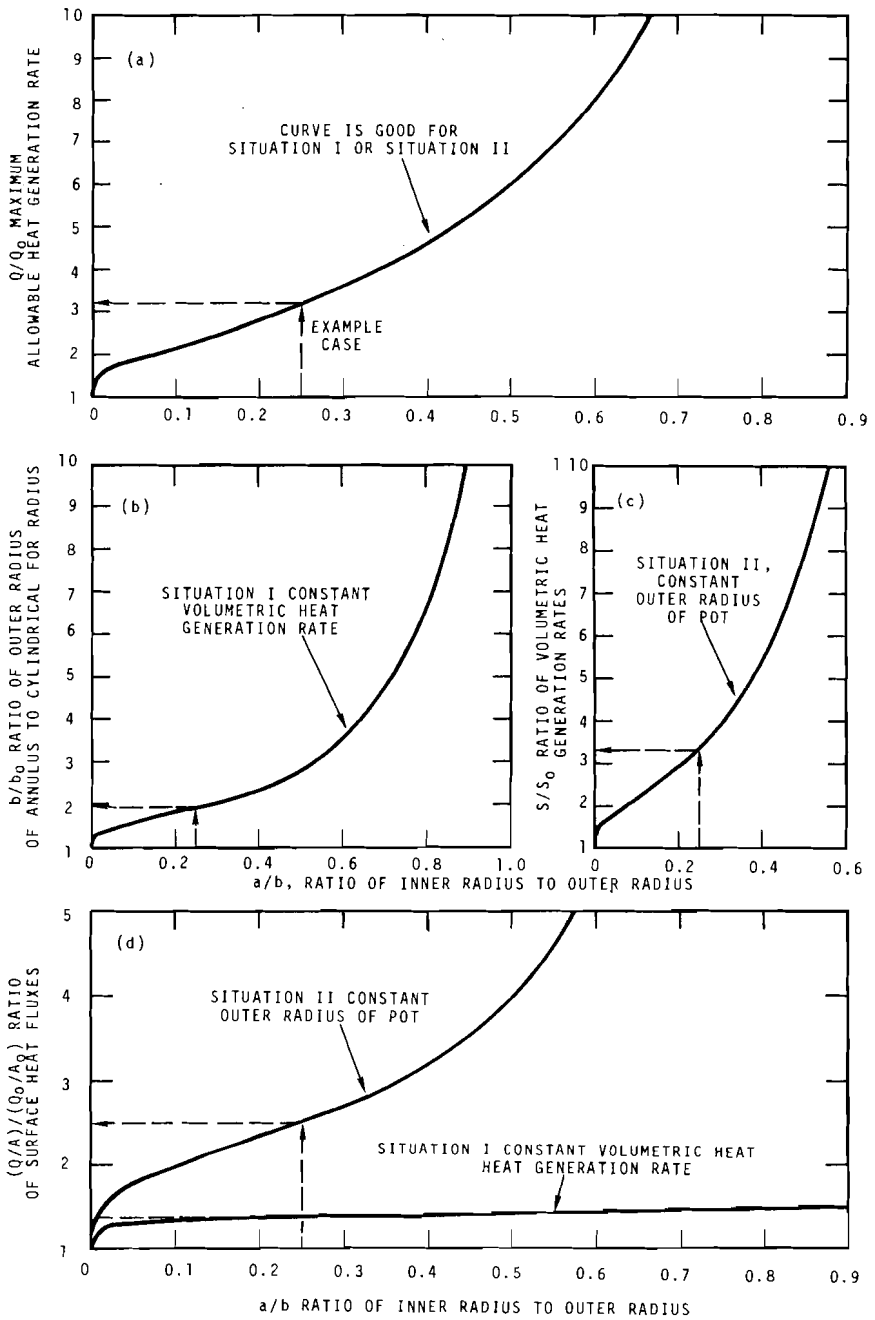

FIGURE 6. Annular Canisters - Constant Radius vs Constant Volumetric Heat Generation Rate

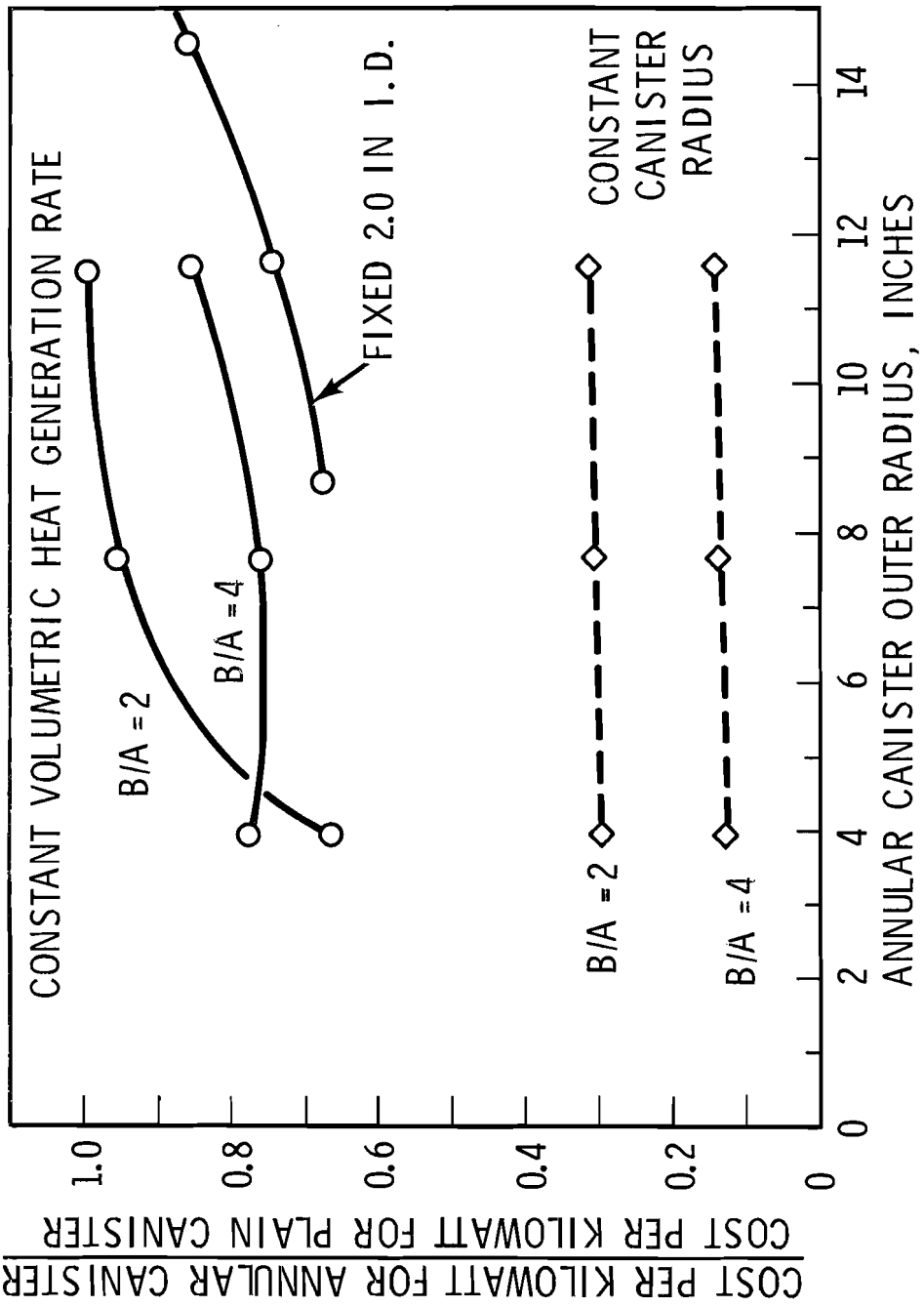

FIGURE 7. Annular Containers - Cost Per Kilowatt for Constant Radius and Constant Heat Generation Rate

waste with k=0.2 Btu/(hr) (ft^2)(°F/ft) and a surface-to-maximum-waste temperature rise of 800°C. There is only a slight cost advantage in terms of cost per kilowatt for annular canisters with constant canister radius. The comparison is relatively independent of the radius of the annular canisters in the region of investigation. Standard pipe sizes were used for both inner and outer walls of the annular canisters; use of non-standard pipe sizes would greatly increase canister costs.

The comparison of cost per kilowatt between finned and plain canisters at constant volumetric heat generation rate is given in Figure 8. To make this comparison, the effect of non-standard pipe size container radius on cost was omitted. Canisters with three fins cost more than plain canisters per kilowatt but 5 fins and 7 fins have an advantage. More than 7 fins seem to be indicated as being still cheaper. In Figure 8 comparison on the basis of fixed canister radius gives an advantage for all the finned canisters.

The number of variables that are present in the cost comparisons are relatively large, resulting in a large volume of tables of results. The range of the waste characteristics considered are presented in Table 3 for annular canisters and in Table 4 for finned canisters. A typical computer printout for finned canisters and constant volumetric heat generation rate is given in Table 5.

Analysis of vendor cost estimates indicates that the fabricated canister cost in dollars per square foot of surface area is relatively constant for each canister type as shown in Table 6. This might be a good basis for estimating costs. The fins and annular canisters seem to be cheaper per square foot than plain canisters for both stainless steel and mild steel, but there are also differences between estimators.

PRODUCT CHARACTERIZATION

Melt Development - Effect of Glass Composition on Leachability - W. A. Ross

The properties of a glass are determined primarily by composition and heat treatment. The properties of greatest importance in waste containing glasses are leach resistance, uniformity, viscosity and stability.

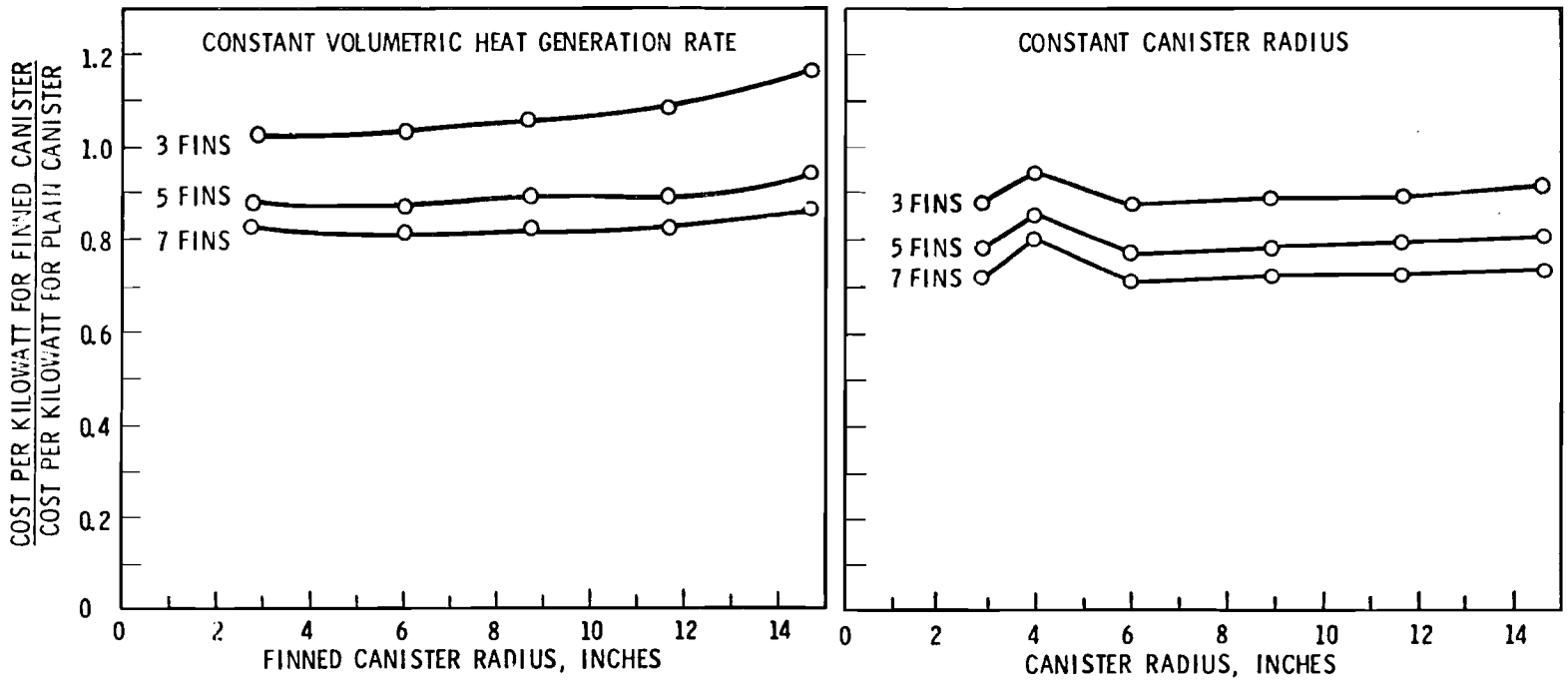

FIGURE 8. Comparison of Cost of Finned Canisters with Plain Canisters at Constant Volumetric Heat Generation Rate and Constant Canister Radius

TABLE 3. Cost Comparison of Annular Canisters With Plain Canisters

Comparison at Fixed Pot Radius

Vendor C, Stainless Annular Pots	k=0.3, ΔT=1800°F
Estimator D, Stainless Annular Pots	k=0.3, ΔT=1800°F
Vendor C, Mild Steel Annular Pots	k=0.3, ΔT=1800°F

Comparison at Fixed Volumetric Heat Generation Rate

ΔT=1800°F

k=0.2	Vendor C, Stainless Annular Pots
k=0.2	Estimator D, Stainless Annular Pots
k=0.2	Vendor C, Mild Steel Annular Pots
k=0.3	Vendor C, Stainless Annular Pots
k=0.3	Estimator D, Stainless Annular Pots
k=0.3	Vendor C, Mild Steel Annular Pots
k=0.7	Vendor C, Stainless Annular Pots
k=0.7	Estimator D, Stainless Annular Pots
k=0.7	Vendor C, Mild Steel Annular Pots

ΔT=1440°F

k=0.2	Vendor C, Stainless Annular Pots
k=0.2	Estimator D, Stainless Annular Pots
k=0.2	Vendor C, Mild Steel Pots
k=0.7	Vendor C, Stainless Annular Pots
k=0.7	Estimator D, Stainless Annular Pots
k=0.7	Vendor C, Mild Steel Pots

TABLE 4. Cost Camparison of Internally Finned Canisters With Plain Canisters

Comparison at Fixed Pot Radius

Vendor C, Stainless Finned Pots	k=0.3, $\Delta T=1800^{\circ}F$
Estimator D, Stainless Finned Pots	k=0.3, $\Delta T=1800^{\circ}F$
Vendor C, Mild Steel Finned Pots	k=0.3, $\Delta T=1800^{\circ}F$
Estimator D, Mild Steel Pots with Stainless Fins	k=0.3, $\Delta T-1800^{\circ}F$

Comparison at Fixed Volumetric Heat Generation Rate

$\Delta T=1800^{\circ}F$

k=0.2	Vendor C, Stainless Finned Pots
k=0.2	Estimator D, Stainless Finned Pots
k=0.2	Vendor C, Mild Steel Finned Pots
k=0.2	Estimator D, Mild Steel Pots with Stainless Fins
k=0.3	Vendor C, Stainless Finned Pots
k=0.3	Estimator D, Stainless Finned Pots
k=0.3	Vendor C, Mild Steel Finned Pots
k=0.3	Estimator D, Mild Steel Pots with Stainless Fins
k=0.7	Vendor C, Stainless Finned Pots
k=0.7	Estimator D, Stainless Finned Pots
k=0.7	Vendor C, Mild Steel
k=0.7	Estimator D, Mild Steel Pots with Stainless Fins

$\Delta T=1440^{\circ}F$

k=0.2	Vendor C, Stainless Steel
k=0.2	Estimator D, Stainless Steel
k=0.2	Vendor C, Mild Steel
k=0.2	Estimator D, Mild Steel Pots with Stainless Fins
k=0.7	Vendor C, Stainless Steel
k=0.7	Estimator D, Stainless Steel
k=0.7	Vendor C, Mild Steel
k=0.7	Estimator D, Mild Steel Pots with Stainless Fins

TABLE 5. Cost Comparison for Fixed Volumetric Heat Generation Rate of Stainless Steel Pots With and Without Fins

WASTE IS CALCINE, KO= .20, BTU-FT/(SQ.FT.-HR.-F.)

METAL THERMAL CONDUCTIVITY, K1=26.00, BTU-FT/(SQ.FT.-HR.-F.)

MAX. WASTE TEMP. = 1652. F., POT SURFACE TEMP. = 212.
DELTA TEMP. = 1440. DEGREES FAHRENHEIT.

POT HEIGHT IS 10.0 FEET.

	RADIUS INCHES	FINS	WATTS PER LITER	KILO-WATTS TOTAL	WATTS/ SQUARE FOOT *	$ PER SQUARE FOOT *	COST, $ PER K-W	$ RATIO FINS NO FINS
FINS	2.880	3	324.1	15.68	789.0	41.060	52.04	
PLAIN	2.302	0	324.1	10.60	879.9	44.680	50.78	1.0249
FINS	2.880	5	416.5	19.37	839.4	34.544	41.15	
PLAIN	2.030	0	416.5	10.60	997.5	46.550	46.67	.8819
FINS	2.880	7	508.8	22.70	864.0	31.646	36.63	
PLAIN	1.837	0	508.8	10.60	1102.5	48.244	43.76	.8371
FINS	3.991	3	164.6	15.55	564.5	37.854	67.06	
PLAIN	3.229	0	164.6	10.60	627.2	40.956	65.30	1.0268
FINS	3.991	5	208.5	19.15	598.8	30.995	51.76	
PLAIN	2.869	0	208.5	10.60	705.8	42.045	59.57	.8689
FINS	3.991	7	251.1	22.40	615.2	27.912	45.37	
PLAIN	2.615	0	251.1	10.60	774.5	43.057	55.59	.8162
FINS	6.000	3	70.8	15.33	370.1	36.003	97.29	
PLAIN	4.924	0	70.8	10.60	411.3	38.697	94.09	1.0340
FINS	6.000	5	88.3	18.78	390.5	28.961	74.17	
PLAIN	4.408	0	88.3	10.60	459.4	39.069	85.04	.8721
FINS	6.000	7	105.0	21.89	399.9	25.765	64.43	
PLAIN	4.044	0	105.0	10.60	500.7	39.460	78.80	.8176
FINS	8.625	3	33.4	15.06	253.0	36.121	142.77	
PLAIN	7.170	0	33.4	10.60	282.5	38.276	135.50	1.0536
FINS	8.625	5	41.2	18.33	265.2	28.613	107.88	
PLAIN	6.458	0	41.2	10.60	313.6	38.280	122.07	.8838
FINS	8.625	7	48.4	21.29	270.5	25.097	92.78	
PLAIN	5.955	0	48.4	10.60	340.1	38.341	112.73	.8230
FINS	11.625	3	18.0	14.79	184.4	38.004	206.13	
PLAIN	9.774	0	18.0	10.60	207.2	39.188	189.13	1.0899
FINS	11.625	5	21.9	17.88	191.9	29.050	151.35	
PLAIN	8.849	0	21.9	10.60	228.9	38.655	168.91	.8960
FINS	11.625	7	25.6	20.68	194.9	25.132	128.94	
PLAIN	8.191	0	25.6	10.60	247.2	38.432	155.45	.8295
FINS	14.625	3	11.1	14.56	144.2	43.868	304.21	
PLAIN	12.414	0	11.1	10.60	163.1	42.652	261.44	1.1636
FINS	14.625	5	13.5	17.48	149.2	32.023	214.70	
PLAIN	11.287	0	13.5	10.60	179.4	40.784	227.30	.9446
FINS	14.625	7	15.6	20.13	150.8	26.969	178.82	
PLAIN	10.480	0	15.6	10.60	193.2	39.808	205.99	.8681
FINS	17.625	3	7.5	14.35	117.9	46.664	395.75	
PLAIN	15.085	0	7.5	10.60	134.3	48.630	362.22	1.0926
FINS	17.625	5	9.1	17.12	121.2	35.654	294.13	
PLAIN	13.766	0	9.1	10.60	147.1	45.558	309.67	.9498
FINS	17.625	7	10.5	19.64	122.1	29.265	239.69	
PLAIN	12.815	0	10.5	10.60	158.0	43.450	274.94	.8718

* VERTICAL SURFACES AND ONE SIDE OF FINS IN FINNED POTS.

TABLE 6. Canister Cost in Dollars per Square Foot of Material

STAINLESS STEEL	VENDOR C	ESTIMATOR D
PLAIN	41.59	37.75
FINNED	32.92	24.92
ANNULAR	32.60	40.51
MILD STEEL		
PLAIN	19.52	19.70
FINNED	11.92	--
ANNULAR	11.49	--

Three oxide systems were examined to note effects of composition on leachability. The systems are (1) SiO_2-Al_2O_3-B_2O_3-30 wt% PW-6 calcine, (2) SiO_2-ZnO-B_2O_3-CaO-MgO-30 wt% PW-6 calcine and (3) SiO_2-B_2O_3-Na_2O-CaO-MgO-45 wt% PW-4c calcine.

The glasses in the first oxide system were melted at 1150°C for 3 hr after which observation and measurements were made on the glass. The leach testing was performed by the Soxhlet method for periods of 24 hr. The results of the leach tests are shown in Figures 9 and 10. The glasses tested in Figure 9 were prepared with various amounts of B_2O_3, either 15% or 32% Al_2O_3, SiO_2 to balance and 30% PW-6 calcined oxides which can be subdivided as 8.6 wt% Na_2O, 5.6 wt% Fe_2O_3, 12.5 wt% fission product oxides and 3.3 wt% other oxides. The glasses tested in Figure 10 were constituted similarly except Al_2O_3 was varied while B_2O_3 was held at either 5, 10 or 20 wt%.

Figure 9 shows that there is an optimum content of 5-10 wt% B_2O_3 which the glass should have for minimum leachability. Figure 10 shows that the optimum amount of Al_2O_3 which should be added appears to increase with B_2O_3 concentration. Figures 9 and 10 indicate that to obtain mimimum leachability for system (1) the concentrations of B_2O_3 and Al_2O_3 should be about 5-10 wt% each of Al_2O_3 and B_2O_3. Longer term testing would be required to more accurately determine the minimum. The glasses prepared in this system were also observed for homogeneity and viscosity. As might be expected with the low melting temperature and high Al_2O_3 content, the glasses were very viscous and contained some residual crystals. The higher B_2O_3 glasses had the lower viscosity and best homogeneity of the system.

Due to the problems of viscosity with the first oxide system, work was begun on the second system. The ZnO system is very similar to that developed previously[a] for the PW-4b glasses which form melts of suitable viscosity at 1150°C. The base composition from which individual variations are being made is 31 wt% SiO_2, 23.5 wt% ZnO, 11.5 wt% B_2O_3, 2.5 wt% MgO, 1.5 wt% CaO

(a) Quarterly Progress Report, BNWL-1741, p. 3, April 1973.

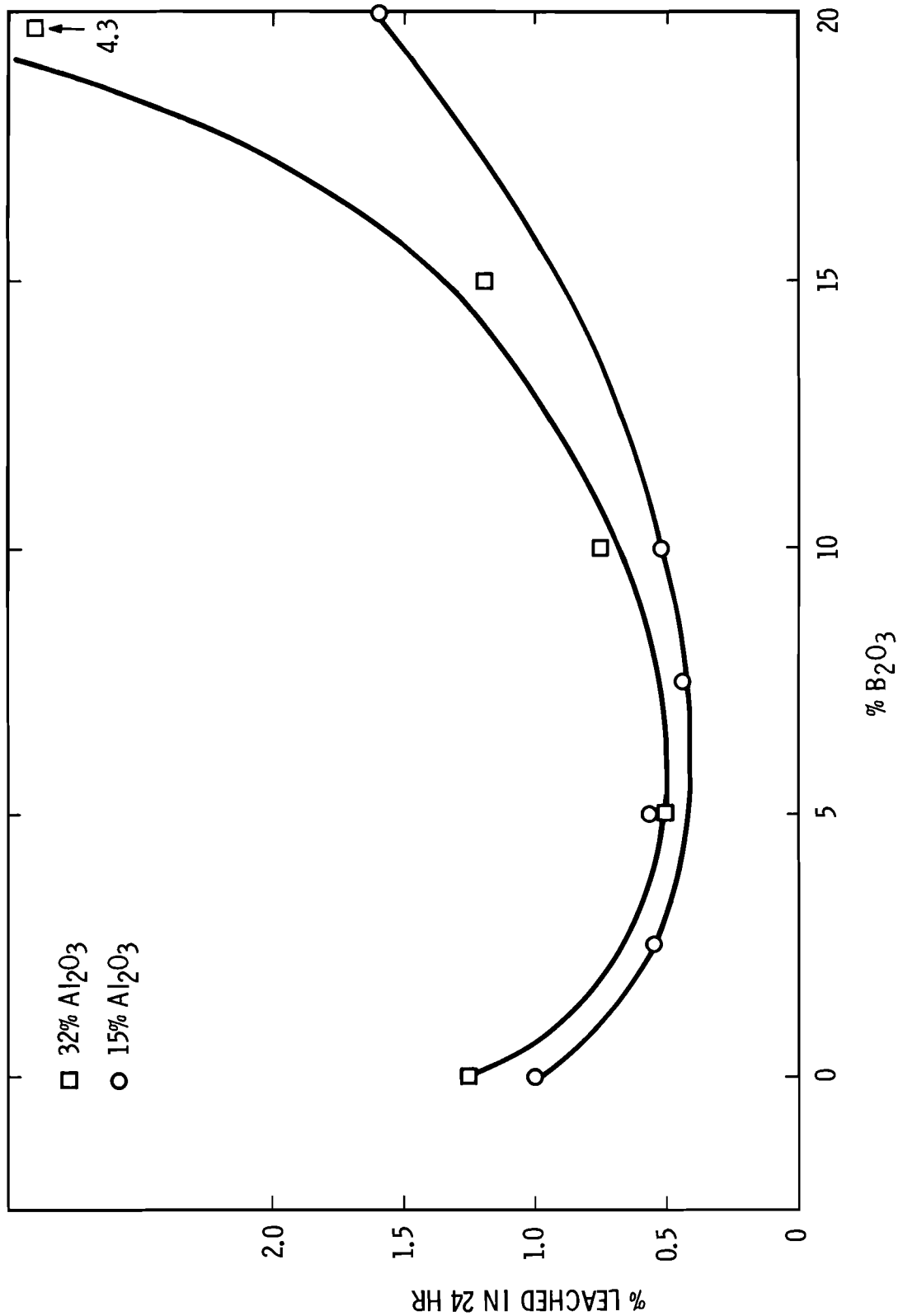

FIGURE 9. Leachability of System SiO_2-B_2O_3-Al_2O_3-30 wt % PW-6 Calcine

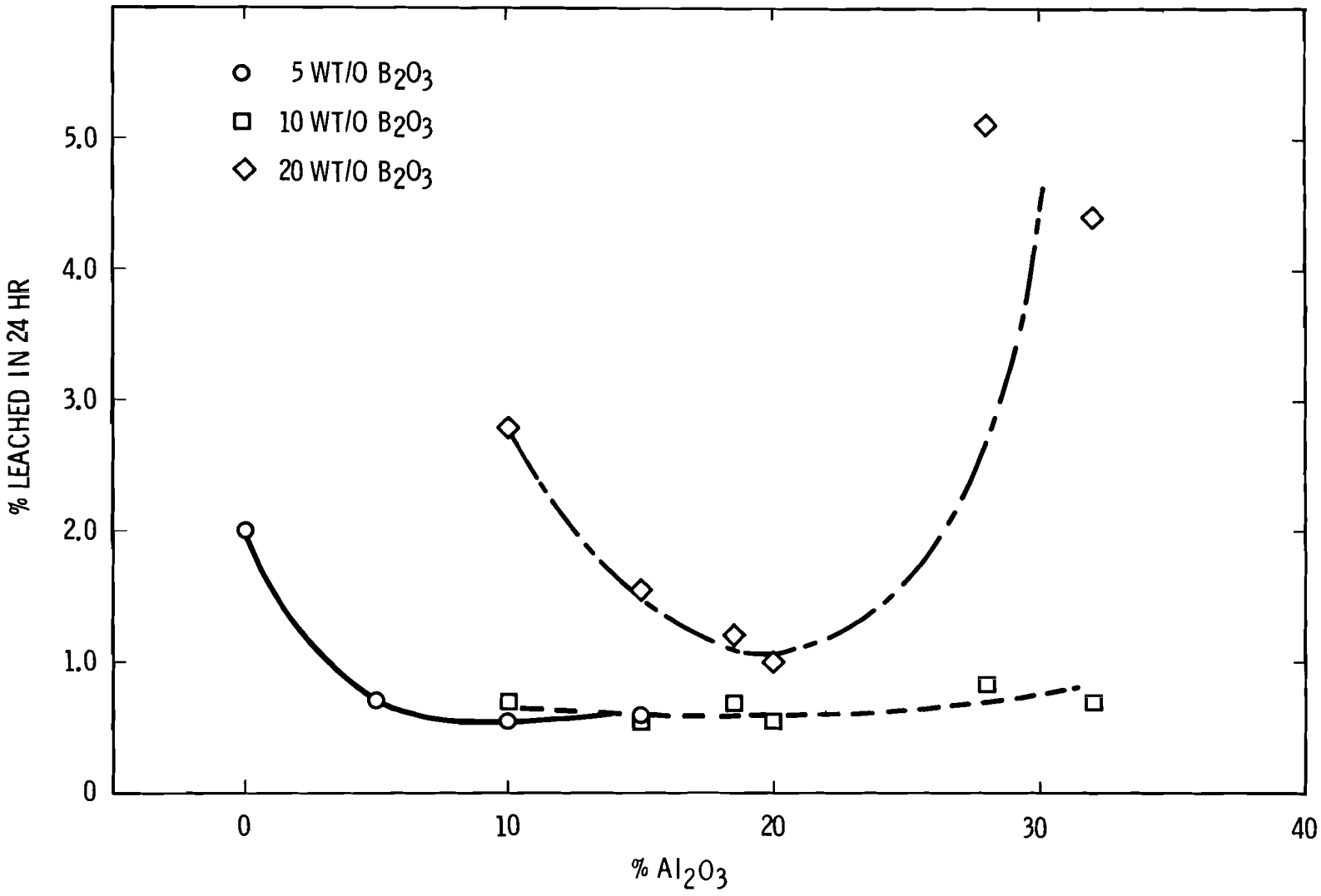

FIGURE 10. Leachability of System SiO_2-B_2O_3-Al_2O_3 - 30 wt % PW-6 Calcine

and 30 wt% PW-6 calcine. The study is in its early stages and only $ZnO-SiO_2$ variations are tested. As can be noted from Figure 11 the indications are that increased ZnO reduces leachability. Longer term tests are being conducted to confirm the indication.

The third system includes PW-4c calcine which is a waste composition calcined on alumina particles and contains about 60-75 wt% Al_2O_3. Due to the high Al_2O_3 content all melts were prepared at 1400°C. The base composition from which individual variations were made contained 5 wt% B_2O_3, 5 wt% Na_2O, and 5 wt% CaO. When MgO was added no CaO was included. The individual oxides were varied with SiO_2. The 24-hr Soxhlet leachabilities are shown in Figure 12. The data show that addition of any of the four oxides increases leachability. The most interesting part of the data is that Na_2O and B_2O_3 apparently increase leachability less than CaO or MgO. Oxide contents of greater than 5 wt% CaO, MgO, Na_2O or B_2O_3 also appear to greatly increase leachability and should therefore be avoided. B_2O_3 content was not varied as widely in this test as in first system (Figure 9) but should behave quite similarly as both have about 32% Al_2O_3. Most glass prepared from this system contained some residual particles, probably Al_2O_3. The amount of the residual particles decreases with increased additions of any of the additives. It therefore appears that leachability and homogeneity are opposing criteria and the final composition must be a balance of the two properties.

Characterization of Crystallites in PW-4b Melts - W. A. Ross

The PW-4b melt composition 72-68 [a] when formed rapidly and in small quantities appears to be homogenious to the eye. Melting of larger quantities and more detailed examination show crystallites are dispersed throughout the glass. At least two crystalline phases can be observed due to their large difference in size. Some residual bubbles or pores can also be observed as black spots.

This study was undertaken to identify the character and origin of the crystallites. Methods used in the study included metallography, x-ray

(a) Quarterly Progress Report, BNWL-1761, p. 4, April 1973.

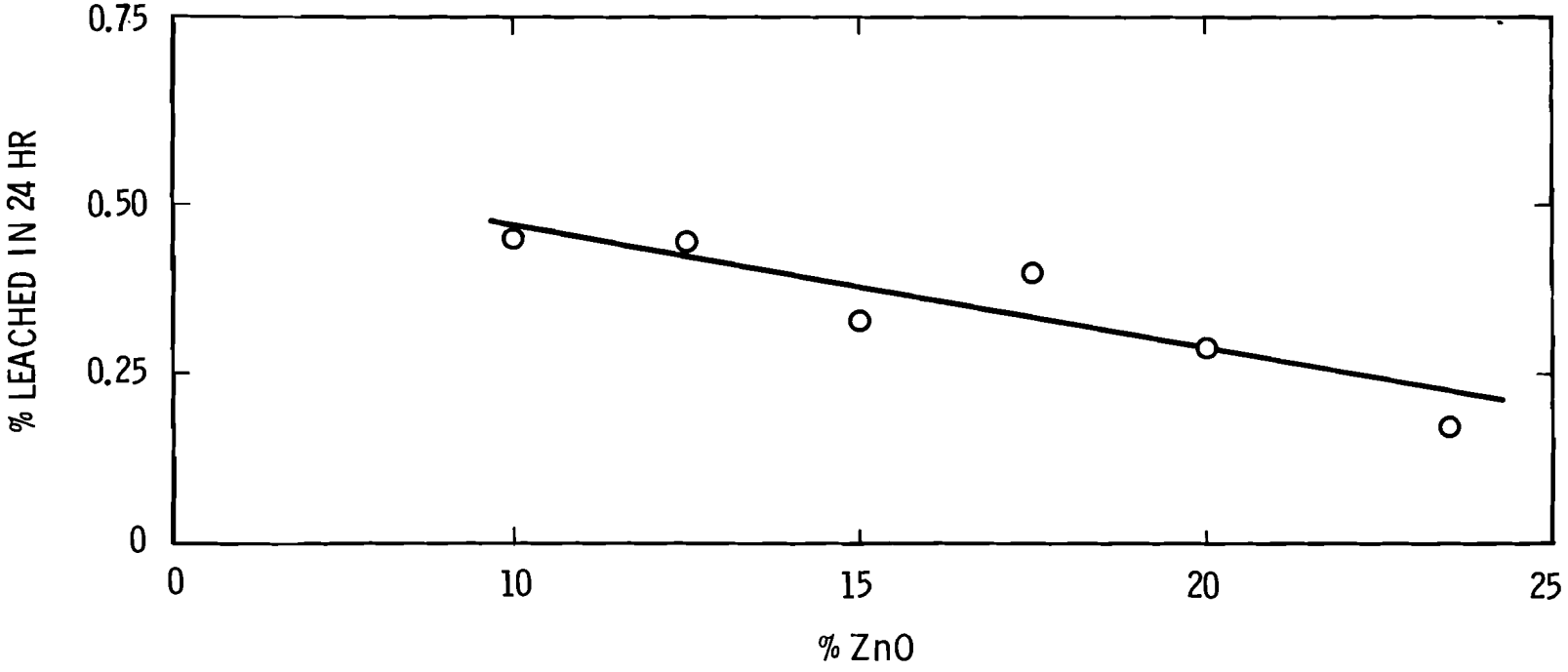

FIGURE 11. Leachability of System SiO_2-ZnO - 11.5 wt% B_2O_3 - 2.5 wt% MgO - 1.5 wt% CaO - 30 wt% PW-6 Calcine

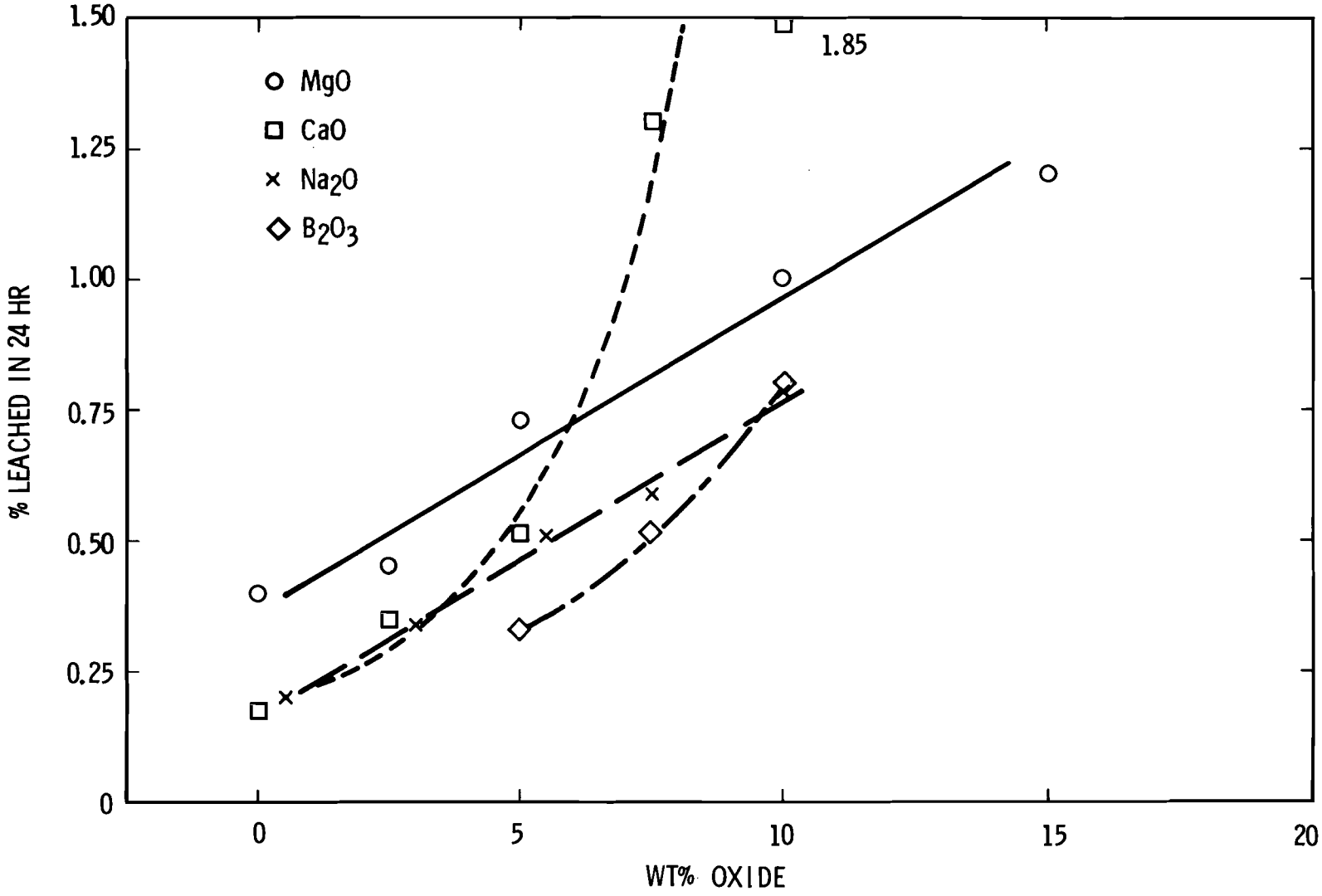

FIGURE 12. Leachability of the System SiO_2-B_2O_3-Na_2O-CaO-MgO - 45 wt% PW-4c Calcine

diffraction, and microanalysis with the Scanning Electron Microscope (SEM). Metallorgraphy shows that the crystallites are of several types (Figure 13). The gray matrix is glass.

X-ray diffraction and the SEM were successfully used to identify the crystalline phases. Figures 14 and 15 are micrographs obtained with the SEM. Figure 15 is higher magnification of the area outlined in Figure 14. At the higher magnification, it becomes apparent that the fine bright phase is individual crystals which have agglomerated. The estimated crystal size is of the order of 1 μm. X-ray fluorescence patterns were obtained on the three crystals identified by arrows in Figure 15. The upper crystal is primarily Fe, Cr, Ni, and possibly Zn, although the Zn may have been from the glass matrix. This type of crystal is probably the spinel structure observed in the x-ray diffraction patterns.

The crystal identified by the arrow near the center of the micrograph was identified as primarily cerium with some matrix background. One type of x-ray diffraction patterns observed was similar to either a CeO_2 or a rare earth zirconate structure. The SEM data confirms the CeO_2 type crystals, which were also observed in the calcines prepared in the laboratory. Apparently CeO_2 is not completely soluble at the temperatures used to process the present PW-4b glass, although it does have a finite solubility as it was observed in the matrix glass.

The largest crystals observed in both Figures 13 and 14 and noted by the arrow near the bottom of Figure 15 appear to be zircon ($ZrSiO_4$). Zirconium and silicon were the dominant elements observed from the SEM data and one strong $ZrSiO_4$ peak was noted in the x-ray diffraction data. Since zirconium is in the calcine and silicon is in the frit, the zircon crystals must form in the melter. The x-ray diffraction results would also indicate that in the sample examined, the CeO_2 type structure is the predominant type crystal form and is much higher in concentration than the spinel or zircon type crystals.

One additional interesting feature which can be noted in Figure 16 was also observed. This is a possible phase separation which may be occurring

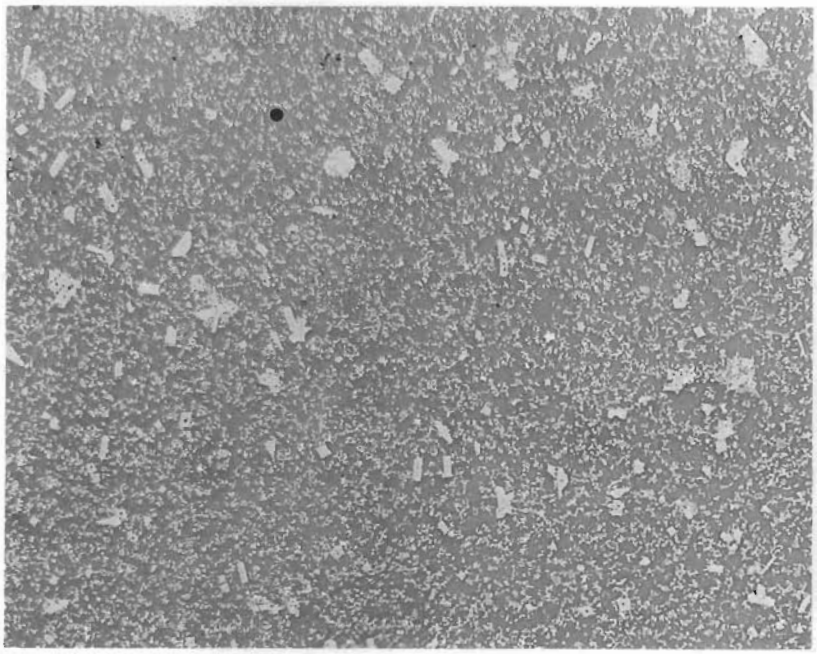

FIGURE 13. 100X Photomicrograph of "Second" Phase Area in PW-4b Type Glass

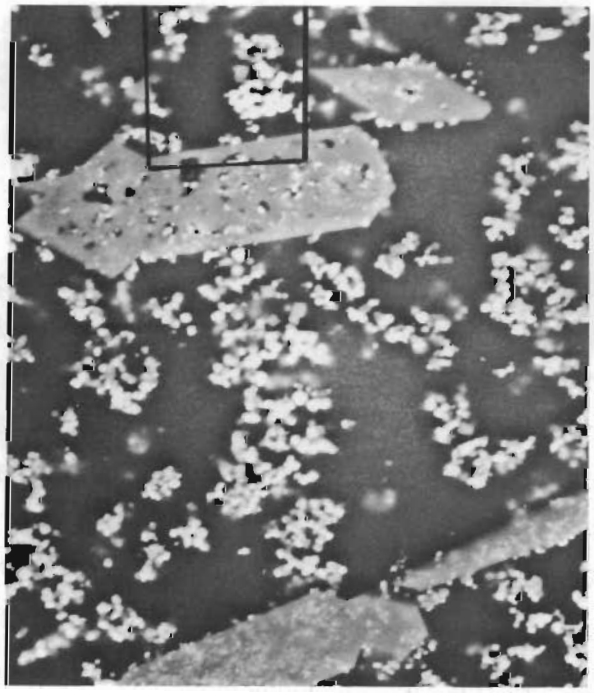

FIGURE 14. 1000X Scanning Electron Micrograph of "Second" Phase Area in PW-4b Type Glass

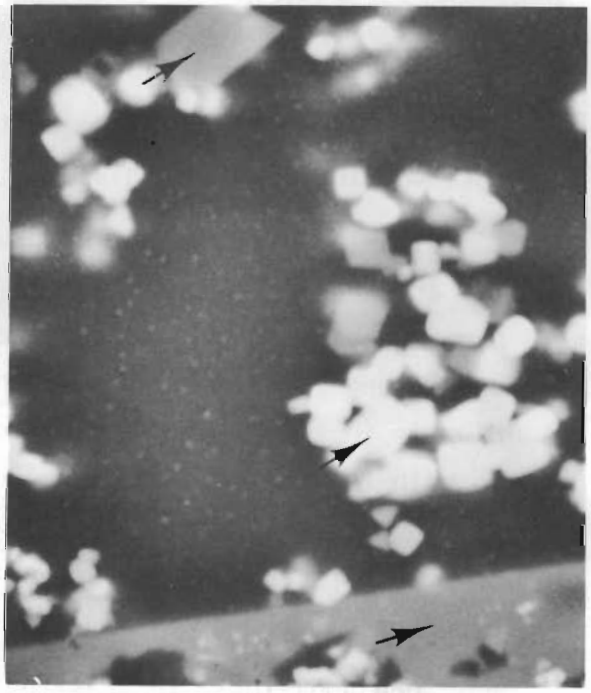

FIGURE 15. 4000X Scanning Electron Micrograph of Outlined Area in Figure 14. Arrow Note Areas Analyzed by X-ray Fluorescence for Elemental Composition

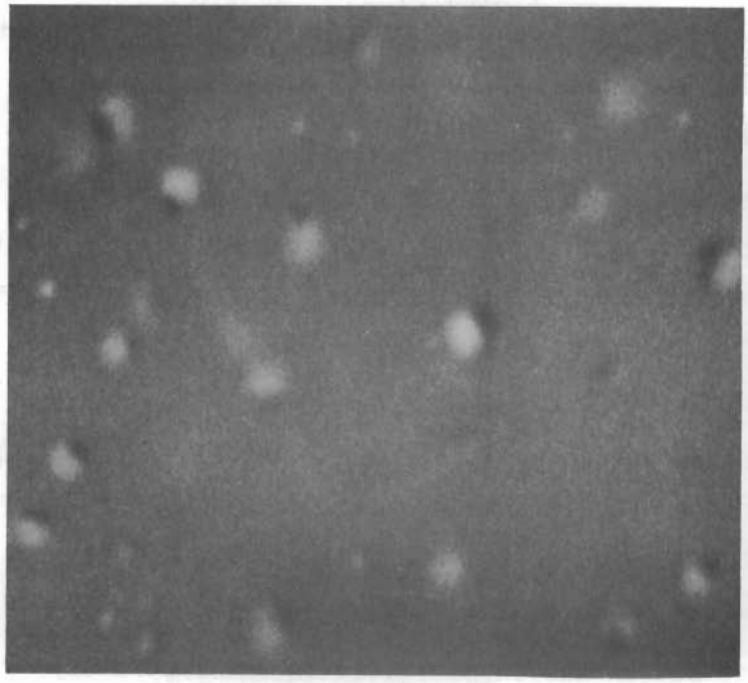

FIGURE 16. 20,000X Scanning Electron Micrograph of Matrix Area of the "Second" Phase from PW-4b Type Glass. Nonhomogeneity Suggests a Possible Phase Separation of the Glass Matrix.

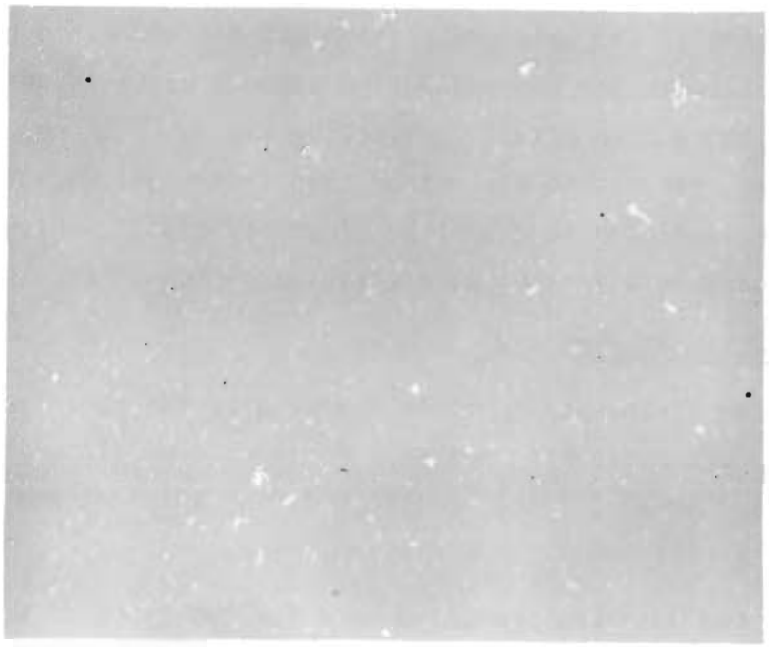

FIGURE 17. 100X Photomicrograph of Glass Sample from Melter Run DSS-8. At Least Two Crystal Phases Appear to be Present.

in the glass during cooling. A comparative analysis of a white spot and matrix showed some difference in the silicon/zinc ratio but no other difference was noted.

Leach testing of second phase areas such as in Figure 13 do not show a significant difference from the bulk material. This might be expected since the continuous phase and the phase most likely to be exposed for leach testing would be the bulk glass phase.

To reduce or eliminate the effects of the crystallites several options can be considered including: (1) increasing the melter temperature, (2) agitating the melt to prevent settling of the crystals, (3) modification of the melt composition to promote greater CeO_2 solubility, and (4) reducing the concentration of the calcine and its associated CeO_2 in the glass.

The first option was investigated in the laboratory by heating melts to 1150, 1200 and 1250°C. Comparison of the melts showed that the crystal phases were sharply reduced at 1200°C and nearly eliminated at 1250°C. Agitation of the melt was successful in dispersing the crystals as can be seen in Figure 17, but it does not appear to aid in dissolving them.

Modification of the melt composition was not attempted because the CeO_2 concentration in the nonradioactive standin waste is nearly double that which will be present in actual radioactive waste. This results from the use of a natural rare-earth mix rather than individual additions of the much more expensive separated rare earths. Tests of glasses which will contain more typical concentrations of rare earths are planned for the next quarter.

Waste Vaporization Studies - W. J. Gray

The purpose of this study is to investigate the vaporization behavior of fission product containing wastes. Accident conditions involving high temperatures and breach of the container during shipment and storage are of particular interest.

Vaporization data are presented here for two types of wastes; fluidized bed PW-4b calcined waste and the waste-containing borosilicate glass 72-68, (BNWL-1761, p. 4) hereafter referred to as PW-4b and 72-68 respectively. All samples were heated in a platinum crucible in a flowing stream of dry air

(3.5×10^{-3} mg of water per liter of air). The cross sectional area of the cylindrical platinum crucible was 1.98 cm^2 in all cases. Sample weight-loss rates were found to be independent of air flow rate at least over the range 1 to 3 ft^3/hr STP; a flow rate of 1 ft^3/hr STP was used in most cases.

Waste PW-4b readily absorbs and desorbs moisture from the room atmosphere. To prevent weighing ambiguities, therefore, this material was maintained in an atmosphere of constant relative humidity (∿38%) prior to heating and in a vacuum desiccator while cooling upon removal from the furnace. All weighings were then made rapidly upon removal of the sample from the desiccator or constant humidity atmosphere.

The amount of water and nitrogen oxides in PW-4b was established as 1.68 wt% and was found to be independent of sample mass. This was determined by heating samples in vacuum at 500°C to constant weight. Actually, most if not all the H_2O and NO_x was lost at temperatures as low as 300 to 400°C and the same results were obtained by heating in dry air at 500°C as were observed by heating in vacuum. Finally, there was no evidence of any loss from these samples other than H_2O and NO_x at temperatures up to 500°C.

Figure 18 shows the weight loss for PW-4b at various temperatures; all samples were the same size. The two typical runs at 1200°C show that the reproducibility is good. Figure 19 shows data at 1200°C for samples of different thickness. The rather abrupt slope changes near 15% weight loss for the thinner samples apparently indicate that the vaporization of some component is near completion. The curve for the thinnest sample shows another change in slope near 17%.

The data shown in Figure 19 indicate that the rate limiting factor is diffusion of the vapor through the powdered sample rather than vaporization from the individual particles. However, because these data apply to the as-calcined material rather than the fluidized-bed calcined material which is deposited on alumina particles, it is not possible to use these data to predict vaporization behavior for thick samples of the latter.

Vapor from a 0.64 cm thick sample of PW-4b heated at 1200°C was deposited on a water-cooled cold finger and quantitatively analyzed by x-ray

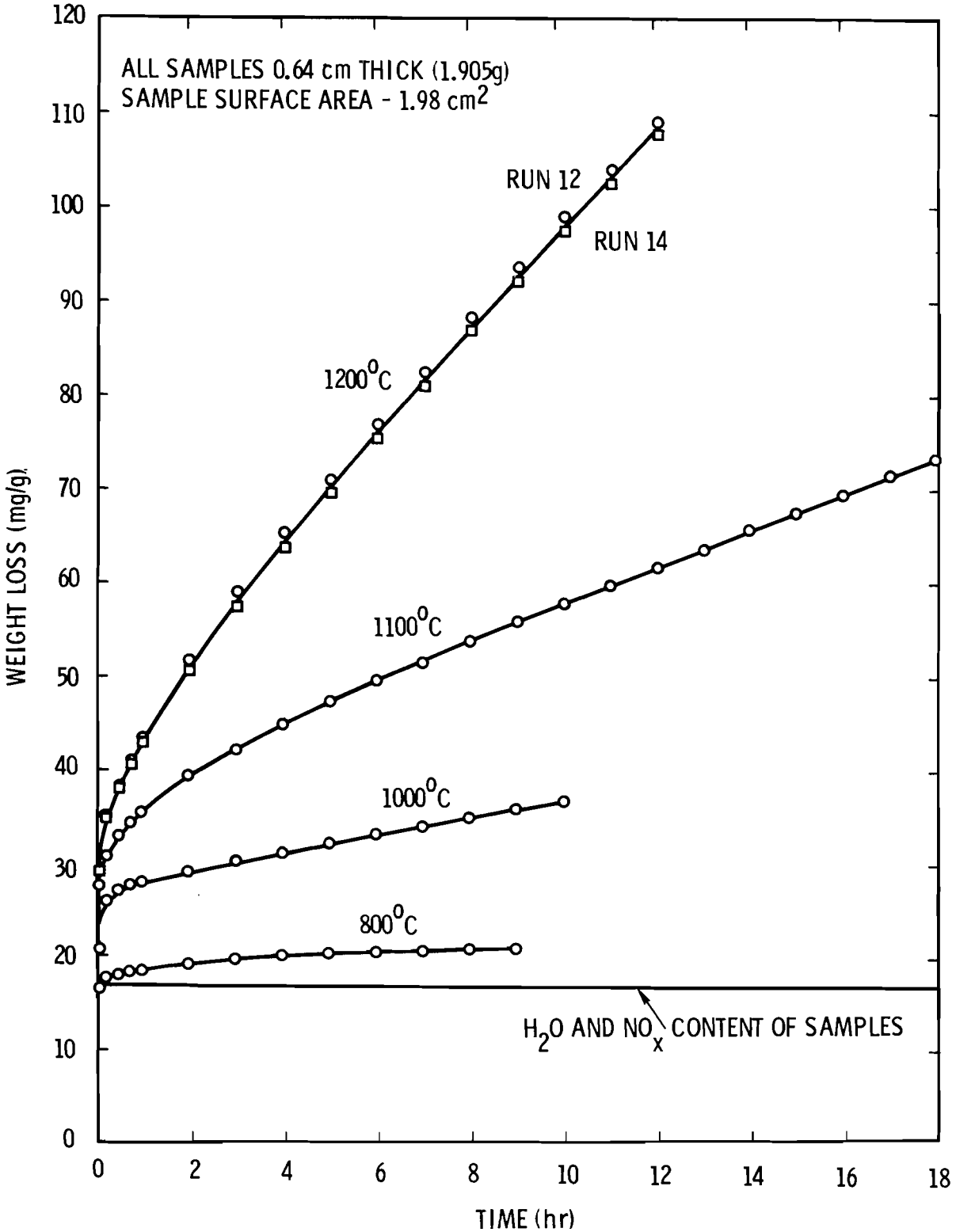

FIGURE 18. Volatilization Weight Loss from PW-4b Calcine

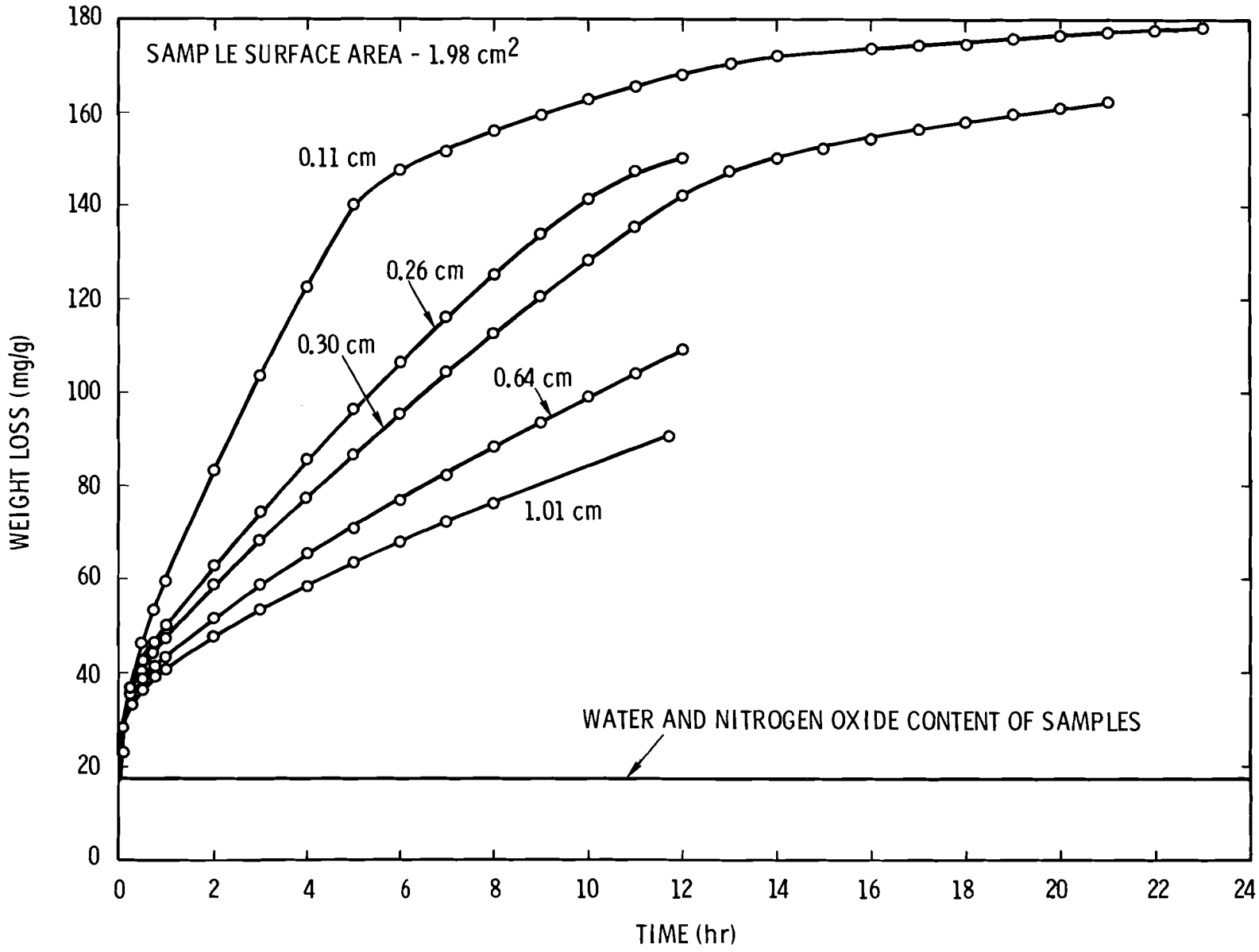

FIGURE 19. Volatilization Weight Loss of PW-4b Calcine Samples of Different Thickness at 1200°C

fluorescence. Two samples were taken; one from the first 30 min of heating and the second for the period between 2 and 6 hr of heating at 1200°C. Results are shown in Table 7. It should be emphasized that these results are preliminary and no attempt will be made here toward interpretation.

Figure 20 shows weight-loss curves for 0.16 cm thick samples of waste 72-68 at various temperatures. Figure 21 shows data at 1200°C for 72-68 samples of different thickness.

TABLE 7. X-ray Fluorescent Analyses of Vapor Deposits From a 0.64 cm Thick Sample of PW-4b Heated at 1200°C

	Fractional wt% of the Volatilized Material[2]	
Element[1]	1st 1/2 hr	2-6 hr
Fe	0.18	0.21
Rb	0.10	0.75
Mo	5.2	9.2
Ru	12.6	33.1
Ag	0.45	0.18
Cd	2.3	3.4
Te	21.7	18.9
Cs	19.5	17.8
	61.9[3]	83.5[3]

Notes: 1) Other elements presented in PW-4b were not detected in the vapor deposit. Detection limits are 0.1% or less.

2) Accuracy is ∿ ± 10% of the values listed.

3) Oxygen cannot be detected but is expected to make up most of the difference to 100%. NO_x and H_2O may also contribute to the difference. This is to be resolved.

Figure 22 shows the effect of sample thickness on weight-loss rates at 1200°C for both PW-4b calcine and 72-68 glass. For PW-4b, weight-loss rates were taken as the average slope of the curves in Figure 19 between 2 and 10 hr (between 1 and 5 hr for the thinnest sample). For 72-68, weight-loss rates were taken as the average slope of the curves in Figure 21 for the

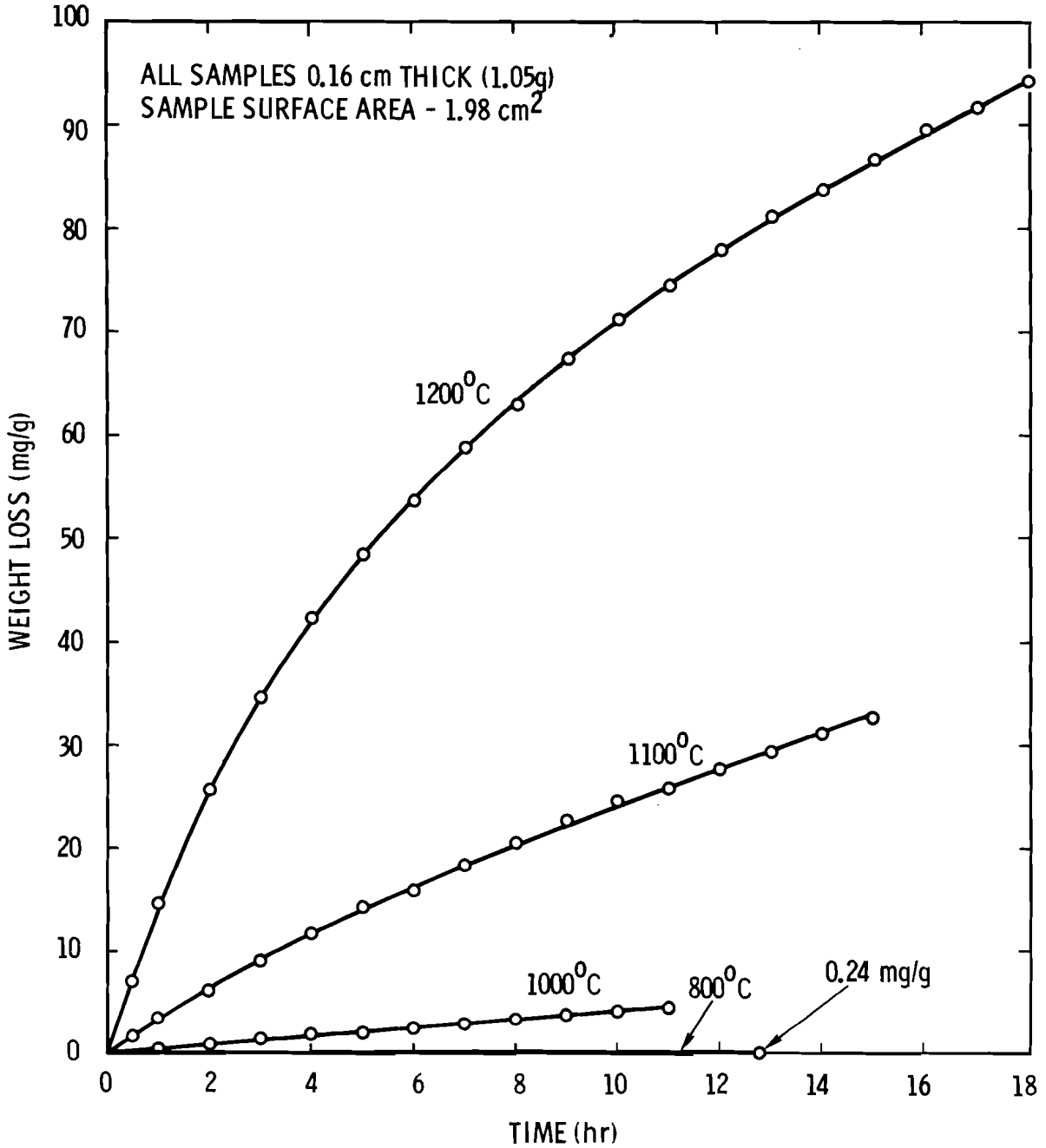

FIGURE 20. Volatilization Weight Loss from Composition 72-68 Borosilicate Glass

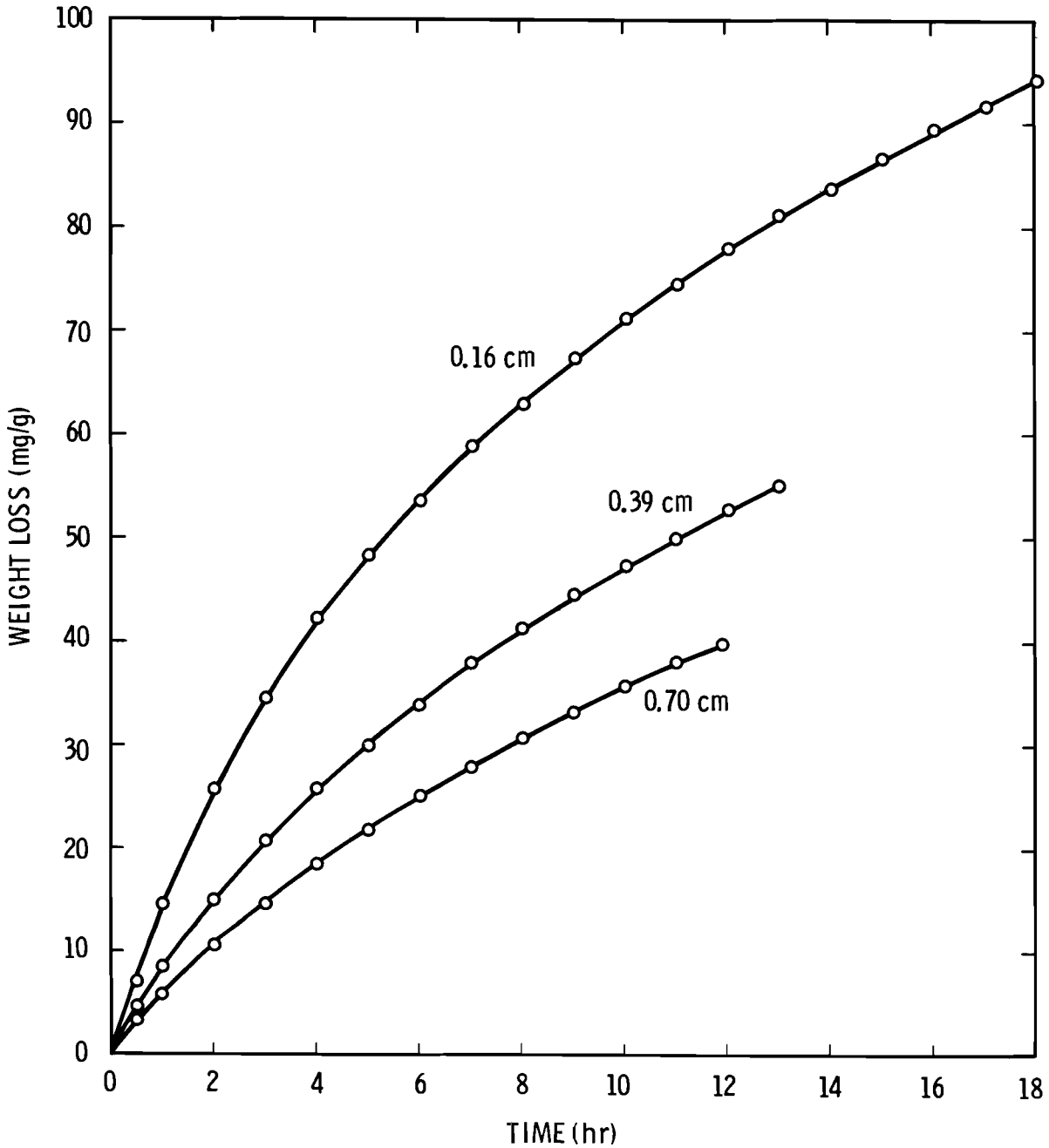

FIGURE 21. Volatilization Weight Loss from Composition 72-68 Samples of Different Thickness at 1200°C

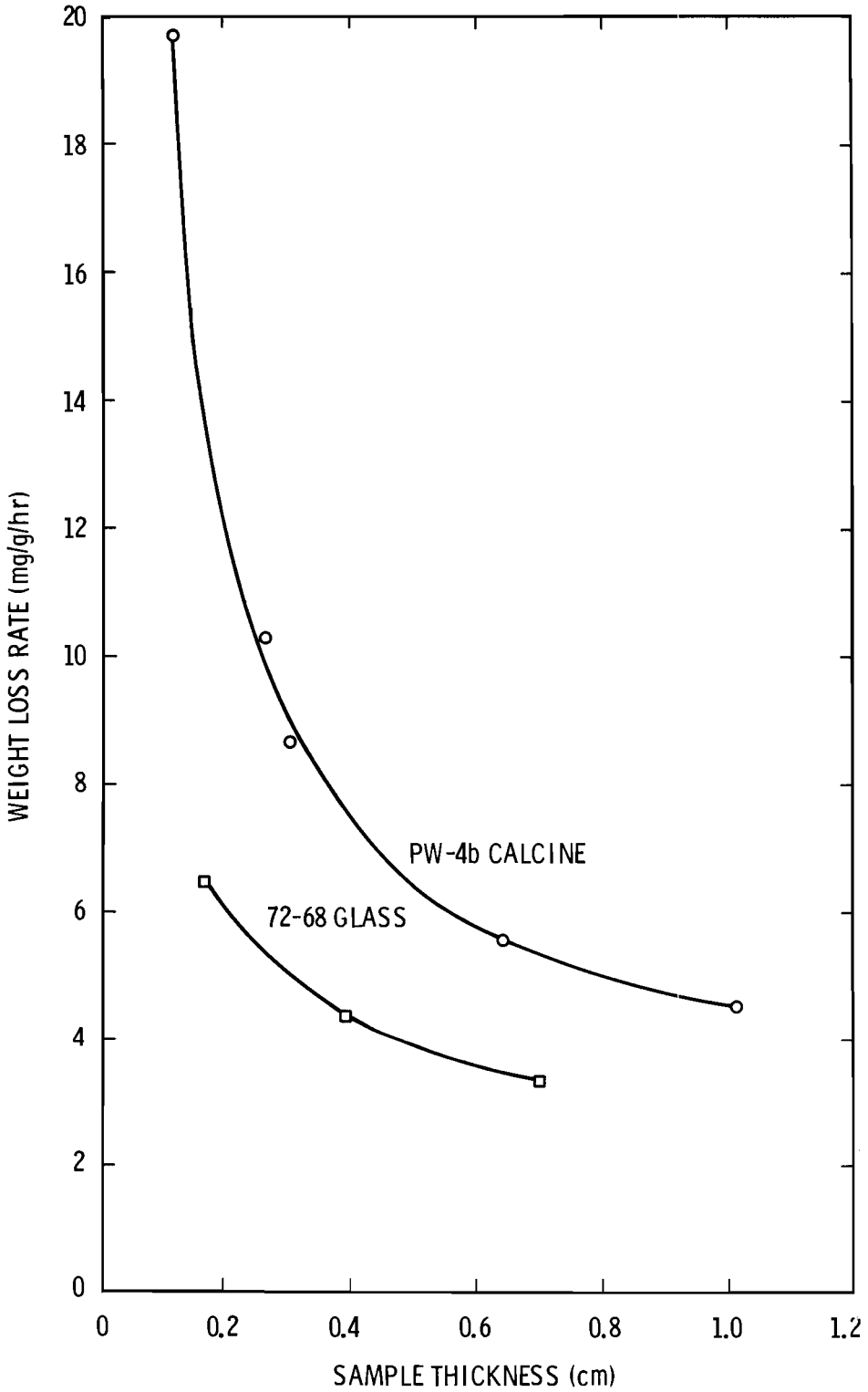

FIGURE 22. Volatilization Weight Loss Rate vs. Sample Thickness

first 12 hr. While Figure 22 shows the weight-loss rates of 72-68 are only about a factor of two less than for PW-4b, a large fraction of the weight loss for 72-68 may be due to the glass frit additive. If so, vaporization of the fission products from 72-68 may be substantially less than for PW-4b.

Helium Generated Stresses and Bubbles in Waste Glass - W. A. Ross and D. F. Newman

Helium gas formed by alpha particle emission from actinide nuclides in high-level waste glasses can produce large internal stresses in the glass.[a] In a perfect glass, gas atoms probably occupy individual interstitial positions. The internal stress or gas pressure which can be contained on this atomic level can be very high. This was demonstrated by the ability of Faile and Roy[b] to produce glass samples saturated with gas at 120,000 psi. Waste glasses with residual crystallites and pores may not have the same capability as a more "perfect" glass.

Porosity can provide sites for gas accumulation. To determine the concentration of porosity in a typical waste containing glass, a sample was obtained from the cold pilot plant spray calciner run DSS-8. The sample and its porosity is shown in Figure 23. The cracks in the sample were probably introduced when the sample was chipped from the interior of the 8 in. canister. The pores are the dark circular areas; quantitative measurements show that the porosity is about 0.22% of the sample volume.

The pores act as small pressure vessels into which the helium can diffuse. Within the glass surrounding each pore the gas produces a radial and a tangential or "hoop" type stress.[c] The radial stress, equal to the internal pressure and compressive in nature, is not normally destructive to glass. The tangential stress, approximately P/2 and tensile in nature, is typically the most likely to cause rupture in a glass. Both compressive and

(a) D. F. Newman and D. C. Quimby, "Helium Buildup in Waste Glass," Waste Fixation Program, Quarterly Progress Report, BNWL-1788, October 1973.

(b) S. P. Faile and D. M. Roy, "Solubilities of Ar, N_2, Co_2 and He in Glasses at Pressures to 10 k bars," J. Am. Cer. Soc., vol. 49, [12], pp. 638-643, 1966.

(c) S. P. Timoshenlco and J. N. Goodier, Theory of Elasticity, McGraw-Hill, (third edition), p. 395, 1970.

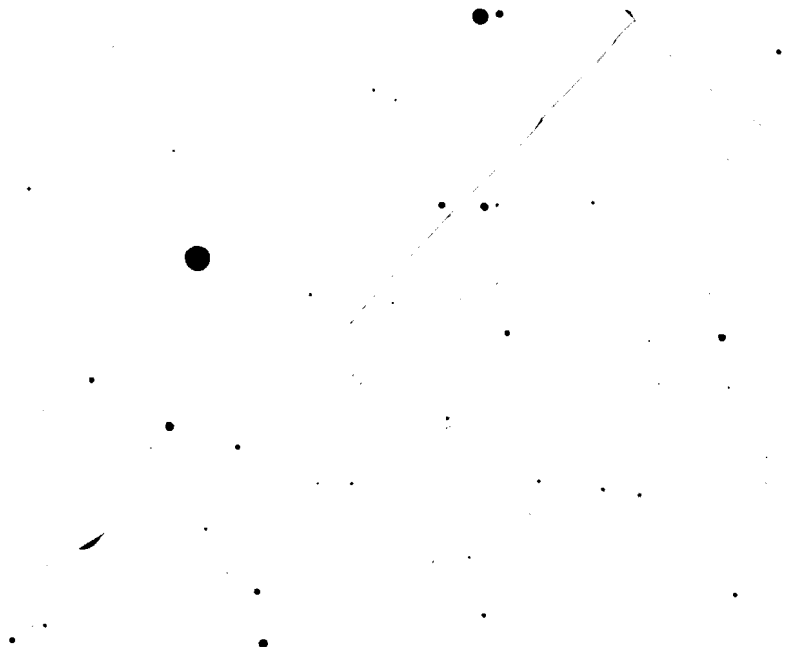

FIGURE 23. 8x Photomicrograph of a Sample of Glass from the DSS-8 Melter Run. Pores or Bubbles can be Noted as the Dark Circular Areas.

tensile stresses are maxima at the glass-gas interface and decrease as $(a/R)^3$, where a is the radius of the pore and R is the radial distance from the pore center to the point of stress in the surrounding glass, assuming the glass is a homogeneous material surrounding an isolated spherical pore.

The localized maximum stresses within the glass near a pore may be much lower than that produced on the atomic level by helium atoms filling individual interstitial positions, but they are more likely to cause rupture of the glass due to the presence of small imperfections and their crack propagation effects. Since there is no significant leakage of helium from glass in a waste canister, the amount of gas in the glass at any time is equal to the cumulative alpha production, and the internal stress of gas pressure is dependent on the volume of porosity within the glass.

The effect of the volumetric porosity on the tensile stress at the bubble-glass interface in 100-year-old high-level waste glass is shown in

Figure 24. The gas pressure in the pores was calculated at a mean temperature of 325°C using the Beattie-Bridgeman equation of state[a] which fits experimental values within 0.15% for densities less than 5 moles per ℓ. As shown in Figure 24, the porosity presently available in the typical sample (∿0.2%) is sufficient to reduce the stress to about 600 psi in the UO_2 fuel waste. The Pu recycle waste would require an increase in porosity to about 3% if the stress is to be reduced to 1000 psi.

If the porosity available is not sufficient as the helium concentration builds within the glass interstitials, additional bubbles may nucleate. The rate of formation of gas bubble nucleation sites is very dependent upon temperature and helium concentration. Faile and Roy (Reference 2) found that nucleation of gas bubbles would occur within 20 hr in a $K_2O \cdot 4SiO_2$ glass at about 250°C with 6.2 mole % argon, but if the argon concentration was reduced to 1.5% temperatures of ∿ 350°C were required for bubble nucleation. They also indicated that higher temperatures were required for nucleation of helium bubbles in the same type glass. The initial nucleated bubble size is very small (in the range of 10-100 Å). Once nucleated, however, bubbles grow in size very slowly unless the glass is at a higher temperature. The minimum temperature required for nucleation and growth in waste glass is not known but temperatures of less than 500°C may be sufficient. The nucleation of new bubbles as well as growth of the new and residual bubbles in the glass could cause the waste to swell into the plenum region of the canister if the temperature and gas concentration are sufficient. The Pu-recycle waste would have the greatest tendency to swell with its higher concentration of gas, while as seen above and from Figure 24, there may be sufficient porosity in the LWR UO_2 fuel waste to accommodate helium and prevent swelling.

Several alternatives could be exercised to accommodate or eliminate the potential swelling of waste glasses due to helium bubble nucleation and growth.

(a) O. A. Hougen, K. M. Watson and R. A. Ragatz, "Chemical Process Principles," Part II, Thermodynamics, John Wiley and Sons, New York, (second edition) p. 563, 1959.

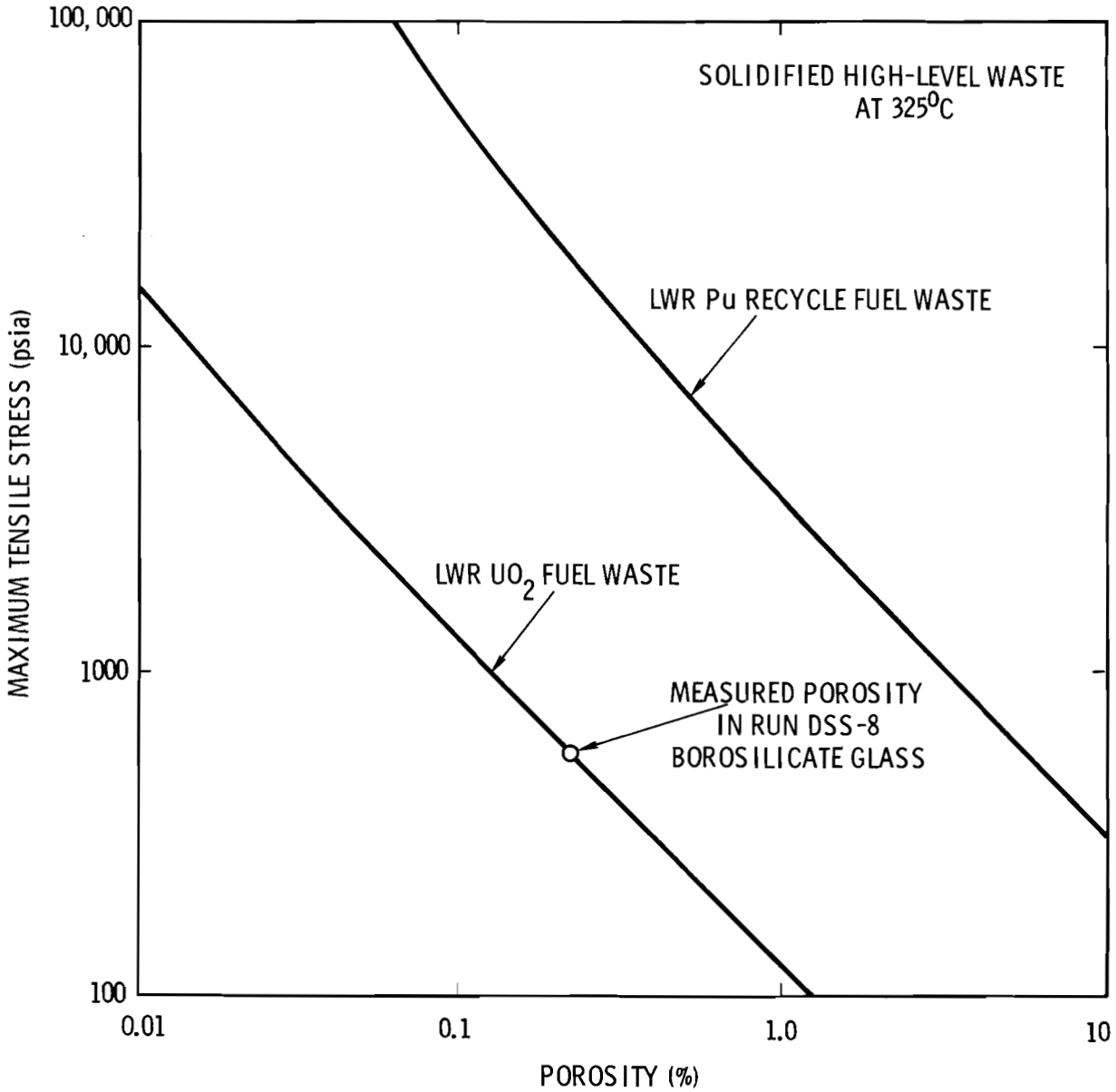

FIGURE 24. Effect of the Volumetric Porosity of Solidified High-Level Waste on the Maximum Tensile Stress Induced by Helium Gas

- The glass specimens could be loaded in a waste canister as an array of close-packed spheres which would have sufficient interstitial voids to accommodate swelling.
- A foaming agent could be added to the glass melt before the waste is poured into its canister and cooled. The large volumetric porosity of the glass could accommodate the helium gas at relatively low pressure.
- The actinide nuclides which produce helium by alpha emission could be separated from the high-level waste that is solidified in glass. The actinides would be solidified in a different matrix than the fission product wastes.

Experiments are planned for waste glasses containing curium, which will provide information about helium induced bubble nucleation and growth. This experimental data will be useful for the safety analyses of waste glass canisters used for 100-year storage of high-level radioactive wastes.

Interim Storage of WSEP Radioactive Waste Canisters

Composition of Gas Inside WSEP Canisters - J. E. Mendel

Gas samples were taken from several WSEP waste canisters and analyzed by mass spectrometry. Results are reported in Table 8. All of the canisters contained air when sealed, but after storage, the oxygen in most of the canisters was depleted to varying degrees. Helium and hydrogen were below detectable limits in all cases. Helium was not expected since the concentration of isotopes which decay by alpha emission was very low in the WSEP canister. There was a possibility that small amounts of hydrogen, generated by radiolysis of residual water, could be present, particularly in the canisters containing pot calcine and phosphate glass.

The pot calcine (PC) product contained traces of residual volatiles, some of which are thought to have been tightly bound water. The outgassing of the volatiles interfered with vacuum leak checking of the PC canisters to such an extent that only one PC canister was successfully vacuum leak-checked (after 3 weeks vacuum pumping), and leak checking of many was not even attempted. PC-6 canister, the PC canister which was successfully leak-checked, was found to contain essentially unreacted air. In contrast, most of the oxygen is gone from PC-8, where residual water probably promoted

TABLE 8. Composition of Gas Phase Samples from WSEP Canisters

	Mass Spectrometric Gas Analysis (Mole %)							
Constituent	PG-1	PG-2	PG-3	PG-9	PG-10	PC-6	PC-8	SS-10
CO_2	0.38	2.76	4.51	11.9	0.28	0.20	0.85	0.14
Ar	0.95	1.00	1.07	1.02	0.94	0.94	1.12	1.09
O_2	20.4	12.6	2.01	1.88	20.8	21.2	2.47	10.9
N_2	78.3	81.6	85.2	85.2	77.9	77.7	95.6	87.8
CO	<0.10	<0.10	<0.10	<0.10	<0.10	<0.10	<0.10	<0.10
He	<0.01	<0.01	<0.01	<0.01	<0.01	<0.01	<0.01	<0.01
H_2	<0.01	<0.01	<0.01	<0.01	<0.01	<0.01	<0.01	<0.01
CH_4	<0.01	<0.01	<0.01	<0.01	<0.01	<0.01	<0.01	<0.01
N_2O	ND	2.13	5.09	ND[a]	ND	ND	ND	ND
NO_x	ND	0.01	2.13	ND	ND	ND	ND	ND
Material of Construction	Mild steel	304L SS	Mild steel	304L SS	304L SS	304L SS	304L SS	304L SS
Diameter	12 in.	8 in.	8 in.	6 in.	6 in.	8 in.	6 in.	8 in.
Waste Type.	PG PW-2	PG PW-2	PG PW-2	PG PW-4m	PG PW-4m	PC PW-2	PC PW-4m	SS PW-4m
Storage History	1.5 yr H_2O	1.5 yr H_2O	1.5 yr H_2O	1.5 yr H_2O	2.6 yr amb air[b]	3.8 yr 400°C air	2 yr 400°C air	2.5 yr H_2O[b]
	4.2 yr amb air	4.1 yr amb air	4.1 yr amb air	2.5 yr amb air				
Core Drilled	No	No	No	No	Yes	No	No	Yes
Most Recent Leak Test, atm cm^3/sec	Leaked	1.8×10^{-8}	3.4×10^{-8}	3×10^{-8}	Leaked	5×10^{-8}	____[c]	5.4×10^{-7}

(a) ND = not detected

(b) Since core drilling

(c) Not leak checked because outgassing occurred under vacuum

oxidation reactions, although, as discussed below, the antifoam agent used in this run probably contributed to oxygen depletion also. Some, but a lesser amount of oxidation, also occurred in the SS-10 phosphate ceramic canister.

The five phosphate glass canisters sampled were stored on the floor of A-cell in air at the ambient air temperature. Subsequent leak checks showed two of the canisters had leaks at their thermowells. The gas from these two canisters (PG-1 and PG-10) had the same composition as air, indicating equilibrium was maintained with outside air through the leaks.

In the canisters without leaks the oxygen was depleted and considerable CO_2 was present. The source of the carbon is presumably residual purex solvent degradation products and/or silicone antifoam agent. Antifoam agent was used in run PC-8 and not in run PC-6, and the CO_2 content of the PC-8 gas was 4 times that of the PC-6 gas. Antifoam agent was used in run PG-9 and not in runs PG-2 and 3, and again the CO_2 content was several times higher in the canister from the run in which antifoam agent was used. It may be concluded that decomposition of antifoam agent is a factor in CO_2 formation in both PC and PG canisters.

In the phosphate glass canisters, however, very significant amounts of CO_2 (2.76 and 4.51%) were found in canisters from runs in which the antifoam agent was not used (PG-2 and PG-3). Thus, residual purex solvent must also be present in the phosphate glass canisters. The CO_2 concentration of PG-2 and PG-3 may be compared with those of PC-6 and SS-10, where antifoam was also not used, but where presumably the feed solutions should have contained a comparable amount of residual purex solvent degradation products. The CO_2 concentrations are over a factor of ten lower in the PC and SS canisters. It may be concluded that the "all wet" phosphate glass process tends to preserve the organics whereas the calcination steps of the pot calcine and spray solidifier "burn" the organic almost completely.

Gas samples from two of the phosphate glass canisters contained significant quantities of nitrogen oxide, mostly in the form of N_2O. Obviously, the phosphate glass product from these two runs (PG-2 and 3) contained residual nitrate from the high sodium PW-2 waste. Ample evidence indicates

that the radiolysis of $NaNO_3$ yields $NaNO_2$ and O_2, with only traces of other products, and that $NaNO_2$ is very stable in a radiation field. To obtain the amount of nitrogen oxide present in the PG-2 and 3 gas samples, either rather large amounts of nitrate had to be present, or the products of radiolysis of nitrate in phosphate glass are different from those formed by radiolysis of pure $NaNO_3$.

The evidence indicates the residual organics and nitrate were present in the phosphate glass, which would imply the presence of residual water also, yet no radiolytic hydrogen was found in the canister gas. Possibly the hydrogen combined with oxygen in the high beta-gamma flux within the canister.

ALTERNATIVE WASTE FIXATION SCHEMES

Coating of Waste Calcine - J. L. Bates

The purpose of this study is to develop a waste storage geometry in which the radioactive waste is coated with a nonreactive, impervious coating(s), thereby making the waste resistant to chemical and thermal degredation.

This particular study is to evaluate the feasibility of coating fluidized bed calcine particles with pyrolytic carbon, (PyC) and pyrolytic carbon and silicon carbide (PyC-SiC). PyC has the potential as a coating for fused waste glasses or waste calcine if the coating could be applied and remain impervious to water or gases. The PyC coated particles could also be made resistant to oxidation by coating the PyC with SiC. The PyC and SiC coatings can both provide impervious coatings with good heat transfer properties.

Waste particles produced in a fluidized bed were coated[a] with pyrolytic carbon and with silicon carbide. Approximately 300 grams of calcine were coated with a pyrolytic carbon coating, and 300 grams were coated with pyrolytic carbon and silicon carbide coatings.

(a) Coatings were applied by Gulf Energy and Environmental Systems, San Diego, California.

The coatings were applied using a fluidized bed. The pyrolytic carbon coating started at ∿900°C and was completed at ∿1100°C in successive layers. Methane was used as the carbon source. The SiC coating was applied to the PyC coated particles. An initial coating of SiC was deposited below 1100°C with the final deposition at 1350°C. Silane was used as the silicon source.

The non-coated and coated particles were examined metallographically to determine the structure of the coated waste (Figures 25-27). The calcine waste is coated on crushed α-Al_2O_3 particles which appear to be single crystal (Figure 25). The waste coating thickness varies between 0.0004 and 0.0008 in. (0.001-0.002 cm) thick. It is porous and friable. The Al_2O_3 particles are very irregular in shape with sharp corners. The waste tends to round-off the sharp angles. The estimated average size of the particles coated with calcine is ∿0.0165 cm wide and 0.0315 cm long. The calcine particles were classified before coating to remove fines and oversize particles. Included in the coatings are only those particles which passed a 70 mesh (0.210 mm opening) screen and those retained on a 200 mesh (0.074 mm sieve opening) screen. Although 90% of the calcine used for coating would pass a 100 mesh (0.149 mm opening) screen it would not pass the 200 mesh (0.074 mm opening) screen.

The estimated sizes of the pyrolytic carbon coated particles are 0.0315 cm in width and 0.0445 cm in length. (Figure 26) The carbon coating varies in thickness from 0.004 to 0.006 cm (40-60 microns). The coating appears to be built up in subsequent layers, with some layers exhibiting some porosity.

The carbon appears to be bonded strongly to the calcine with a very slight indication of a reaction layer at the calcine-carbon interface. Metallic looking particles which are found in the calcine layer are not present in the non-coated particles and suggest a possible partial reduction of some elements in the calcine by the carbon at these temperatures.

The SiC coating on the carbon is relatively uniform being about 0.00175 cm (17.5 microns) thick (Figure 27). The average carbon-SiC coated particles are approximately 0.038 cm in width and 0.057 cm in length. A

0.05 cm

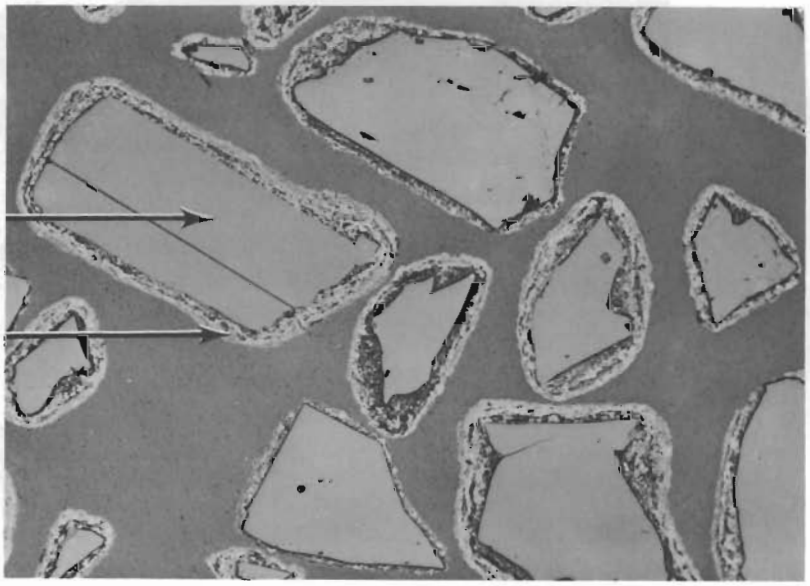

0.016 cm

AVERAGE PARTICLE SIZE: 0.017 - 0.032 cm
WASTE THICKNESS: 0.001-0.002 cm

FIGURE 25. As Coated, Fluidized Bed, Waste Particles

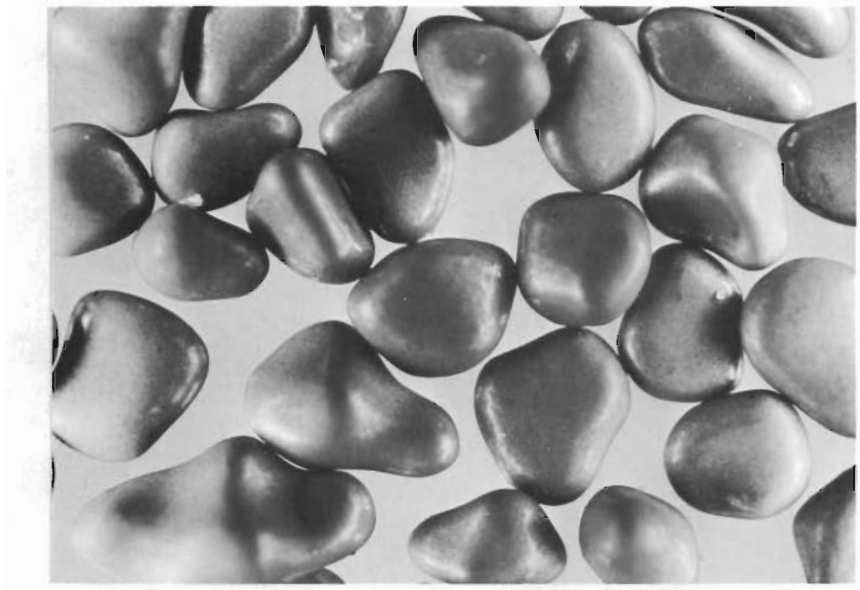

0.05 cm

PYROLYTIC CARBON

WASTE

Al_2O_3

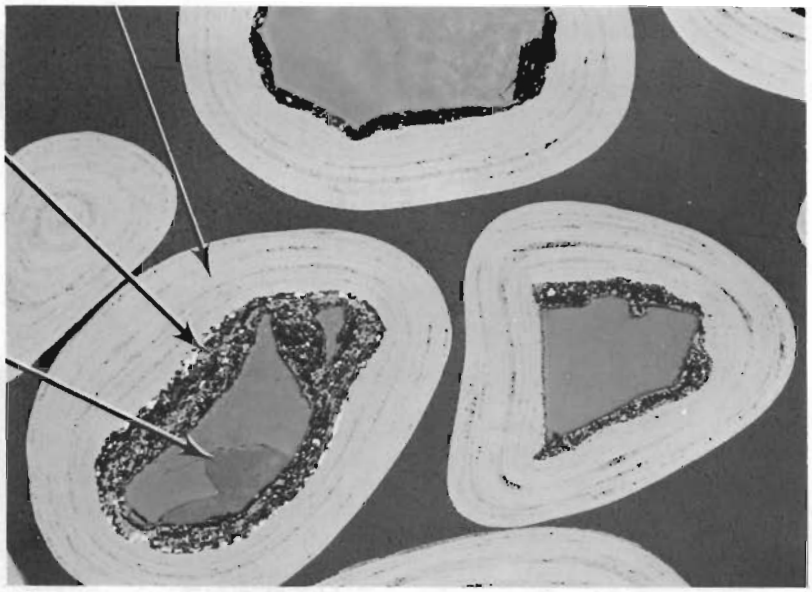

0.016 cm

AVERAGE PARTICLE SIZE: 0.032 x 0.045 cm
AVERAGE CARBON COATING THICKNESS: 0.0005 cm

FIGURE 26. Microstructure of Waste Particles Coated with Pyrolytic Carbon

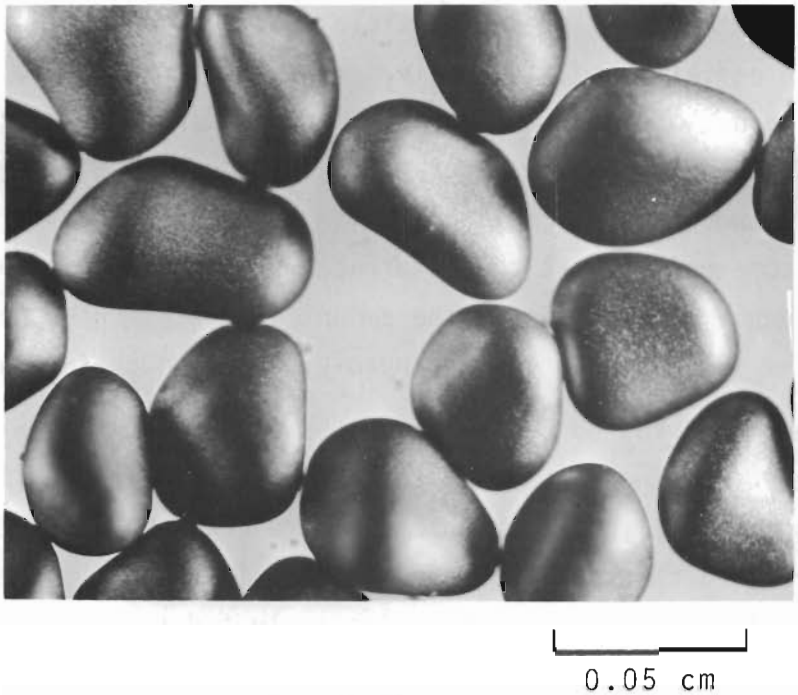

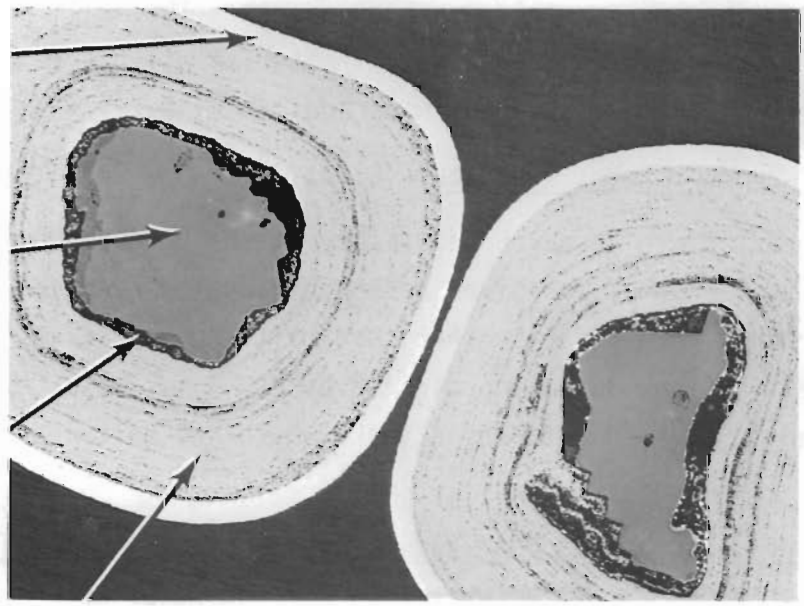

AVERAGE PARTICLE SIZE: 0.038 x 0.057 cm
AVERAGE CARBON COATING THICKNESS: 0.008 cm
AVERAGE SiC COATING THICKNESS: 0.002 cm

FIGURE 27. Pyrolytic and Silicon Carbide Coated Waste Particles

small percentage (2%) of the particle coatings appear to exhibit some cracking, both radially and diagonally. This is attributed to the hard and brittle nature of the SiC coating which was partially fractured during the grinding and polishing procedures required during metallographic preparation. Bonding between the carbon and SiC is generally good with some particles showing some porosity at the interface. The calcine in these particles also show evidence of reduction. The amount of reduction appears to be approximately the same as that for the pyrolytic carbon coated particles.

The carbon coated particles which were coated with SiC were coated separately from those coated with carbon alone. The coating was thicker, being approximately 0.01 cm thick. There was more porosity in the later carbon coating than that observed in the first coating processes. The coated particles are currently being evaluated to determine their physical characteristics, primarily the leach rate. Some of the coated particles will be incorporated in a matrix, such as quartz. This will probably be accomplished by hot pressing. The matrix material will serve as a binder for the particles and will also serve as an additional barrier to dispersion.

Advanced Product Forms Research - G. J. McCarthy, Penn State

The Materials Research Laboratory at the Pennsylvania State University, University Park, PA, was given a subcontract to investigate advanced waste product forms, e.g., forms other than melt-formed glasses or glass-ceramics. The investigation, being coordinated by Dr. G. J. McCarthy, started October 1, 1973, and is divided into three tasks which are described in the following text.

Redundant Protection of Radioactive Wastes (The Russian Doll) - G. J. McCarthy, W. B. White, R. Roy and K. E. Spear

A Russian Doll is the familiar toy in which each doll opens up to reveal another smaller one inside. The term is adopted to represent any multiple barrier protection scheme for radioactive wastes. In the first "layer" of protection, waste ions are substituted into appropriate structures to give highly insoluble products. Subsequent "layers" of protection can mean isolation of these solid solution grains in inert matrices by hot pressing and/or storage of the products in hot pressed cement containers.

The research involves first the selection of candidate low solubility phases based on crystal chemical and thermodynamic parameters. Where relevant data are not available the phases will be synthesized and their leachability determined.

Next, the ability to prepare the phases by adjusting the composition of the liquid or calcined waste with appropriate additions followed by firing will be ascertained. The solid solution limits of the waste ions in the phases for a given temperature and time of firing will be determined using x-ray diffraction as the chief phase analysis tool.

Isolation of Radioactive Wastes in Ceramic Matrices by Hot Pressing - G. J. McCarthy

In a research program at Penn State in 1970-72 supported by the National Science Foundation it was found that by using the ceramic processing technique "hot pressing" or "pressure sintering", a dense, low porosity compact could be made out of mixed powders of radioactive wastes and a suitable matrix. Quartz, one of the least leachable of natural materials, was found to be a particularly desirable matrix.[a] The key element in insuring the inertness of the product is preventing extensive reaction and homogenization of the waste and matrix such as happens in a melt forming process.

The current program is aimed at exploring the feasibility of using this process for an advanced product form. The simulated wastes are the "clean" PW-4b and high sodium PW-6 compositions. Initial efforts will utilize silica as a matrix, added either as crystalline quartz to the waste powder or as silica sol to the waste liquid. Parameters to be varied include temperature and time of waste calcining, hot pressing temperature, time, pressure and waste to matrix ratio. The products will be characterized for degree of waste-matrix reaction, microstructure and chemical homogeneity, porosity and leachability. The latter two tests will be carried out at PNL.

(a) G. J. McCarthy, "Quartz Matrix Isolation of Radioactive Wastes," J. of Materials Science, vol. 8, pp. 1358-1359, 1973.

High Density Hot Pressed Cement Materials in Radioactive Waste Management - D. M. Roy and G. R. Gouda

Cementitious materials having substantially improved properties over those of normal cement and concrete were prepared[a,b,c] using normal cements as starting materials, and could be excellent candidates for nuclear waste storage applications. By employing "hot-pressing" techniques, i.e., moderate pressure at very modest temperatures in the range 100-250°C, strengths an order of magnitude higher (100,000 psi vs. 10,000 psi compressive strength), and porosities an order of magnitude lower (<2 versus approximately 25%) than in normally hardened cement pastes are achieved. Furthermore, the materials have very low permeability, high volume stability, and are relatively stable thermally.

The current research program has as its goal exploring the potential of such materials for Radioactive Waste Management to determine the most desirable combination of materials performance characteristics under the most feasible operating conditions. The possible methods of application envisioned include the following:

- Incorporate solidified wastes, which might be included as "aggregate" (micro or macro) in a "concrete" employing the cementitious material as a matrix binder,
- Form small-moderate size cylindrical specimens with the radioactive waste encapsulated as the core during the fabrication process,
- Use as an outer container of relatively large size, depending on development of fabrication techniques.

The information gained through this research is expected to be important also in other applications of concrete technology to radioactive waste management.

(a) D. M. Roy, G. R. Gouda and A. Bobrowsky, "Very High Strength Cement Pastes Prepared by Hot Pressing and Other High Pressure Techniques," Cement and Concrete Research, vol. 2, pp. 349-366, 1972.

(b) D. M. Roy and G. R. Gouda, "Porosity-Strength Relation in Cementitious Materials with Very High Strengths," J. Amer. Ceram. Soc., vol. 56, pp. 549-550, 1973.

(c) D. M. Roy and G. R. Gouda, "High Strength Generation in Cement Pastes," Cement and Concrete Research, vol. 3, pp. 807-820, 1973.

Crystalline Phase Formation in Calcined PW-6 and PW-4b - G. J. McCarthy

It is important to all of the tasks in this program to know what crystalline phases form on firing the wastes at a particular temperature and duration. Table 9 gives the atomic abundances for PW-6 and PW-4b.

Two approaches are used to suggest what crystalline phases to expect in the x-ray powder patterns after firing. First, data for oxide phases made up of one to three of the major waste cations were collected from the Powder Diffraction File and compared with the observed data. The second approach examined available phase diagrams of two or more of the major waste cation oxides for compound or solid solution formation and thermal stability.

PW-6 calcine, as received from BPNL, had been fired at 500°C for 1 hr. Additional firings of PW-6 were carried out from 750° to 1050°C for 2 to 24 hr. The crystalline phases identified in the products to date (in addition to $NaNO_3$ which was present initially but decomposed at 750°C) are:

- Na_2MoO_4. Cubic spinel structure phase. It first shows up after 2 hr at 750°C and grows in intensity with additional 750°C heat treatment. It is present only in some of the remaining patterns.
- $NaFeO_2$. Orthorhombic β-phase. Present to about the same extent in every firing from 750-1050°C.
- Fluorite[(a)] structure solid solution (F_{ss}). This is the only recognizable phase in "as received" PW-6 except $NaNO_3$. Very broad reflections indicate that it is poorly crystallized. It is a major phase in all firings with the reflections becoming sharper with each higher temperature or time. The composition of this solid solution consists primarily of CeO_2 with, as yet undetermined, amounts of the larger RE^{3+} ions substrating for Ce^{4+} with accompanying oxygen defects. There may also be come ZrO_2 solution in the CeO_2. The unit cell parameter of F_{ss} is approximately ∿5.425Å, slightly larger than 5.411Å for pure CeO_2.

(a) Fluorite is the mineral name for CaF_2. Large cation oxides AO_2 have this structure e.g., UO_2, CeO_2, ThO_2. Pure ZrO_2 has two polymorphs with distorted fluorite structures.

TABLE 9. Atomic Concentrations in Wastes After Initial Drying (in Order of Abundance)

	PW-6		PW-4b
Na	60.5	RE*	27.8
Fe	16.9	Mo	15.4
RE*	6.4	Fe	14.3
Mo	3.5	Zr	13.9
Zr	3.2	Cs	7.1
U	1.9	Ni	4.8
Cs	1.6	Sr	3.6
Ni	1.6	Ba	3.6
Cr	1.4	U	2.6
Sr	0.8	Te	1.6
Ba	0.8	Cr	1.5
Te	0.4	K	1.3
K	0.3	Co	1.3
Co	0.3	P	0.6
P	0.2	Ag	0.3
Ag	0.1	Cd	0.3
Cd	0.1		
	100 atomic %		100 atomic %

* RE = rare earths, chiefly Ce, Nd, La, Pr and Sm

Another fluorite and one or two perovskite structure solid solutions are tentatively identified in the higher temperature firings but these diffractograms are still undergoing investigation.

PW-4b calcines as received, was poorly crystallized and showed only a few very diffuse reflections in the region of fluorite solid solutions. It was fired from 750 to 1400°C for 2 to 24 hr. At the lower temperatures the major reflections in the x-ray patterns are diffuse and can be attributed to two fluorite structure solid solutions. The first, with an a_0 of approximately 5.41Å, appears to be mostly CeO_2 and the second, with a_0 = 5.34Å, could be mostly $RE_2Zr_2O_7$. The cubic cell parameter reported in the Powder Diffraction File for $Nd_2Zr_2O_7$ is 10.64Å (2 x 5.32Å).[a] At the higher

(a) $Nd_2Zr_2O_7$ is reported to have a pyrochlore structure. In this structure type all of the strong reflections can be attributed to a defect fluorite structure with a halved cell parameter.

firing temperatures the two phases react to form a single phase with sharp reflections and a_0 = 5.35Å. Several weak reflections in each of the patterns are not yet assigned to any phase or phases.

Hot Pressing of PW-6/Quartz Mixtures - G. J. McCarthy and M. Davidson

In the earlier Penn State work it was shown that a hard dense compact could be made from equal weights of quartz and the waste PW-4m (similar in composition to PW-4b). Thus, initial effort was on hot pressing PW-6/quartz mixtures.

Since PW-6 is so rich in Na, it was expected that a greater ratio of quartz to waste would have to be used to avoid extensive melting. Available phase diagrams[a] indicate that the first liquid forms in the system Na_2O-SiO_2 at ∿780°C and in Na_2-Fe_2O_3-SiO_2 at ∿760°C. By simply firing pellets of quartz-PW-6 mixtures in air at 1000°C (the hot pressing temperature) it could be determined that a ratio of 3 quartz to 1 PW-6 was necessary to prevent significant deformation of the pellets due to melting. Particulars of two runs using this ratio are given in Table 10.

TABLE 10. 3 SiO_2: 1 PW-6 Hot Pressing Runs

	HP-1	HP-2
Cell	1" graphite	1" graphite
Pressure	3000 psi	3000 psi
Time to Temperature	26 min to 1000°C	18 min to ∿750°C
Time at Temperature	10 min at 1000°C	10 min at ∿750°C
Cooling Time	3 - 5 hr	3 - 4 hr

In HP-1 the densification versus time charts indicated that significant compaction began at ∿750°C so the second run was taken only to this temperature. It is likely that a small amount of a liquid phase is forming at about this temperature and is responsible for the bonding between waste and matrix. This will be considered in interpreting upcoming electron microprobe and scanning electron microscope measurements.

(a) E. M. Levin, C. R. Robbins and H. F. McMurdie, "Phase Diagrams for Ceramists," American Ceramic Society, Columbus, Ohio, 1964 and 1969.

HP-1 was hard and dense and compared favorably with quartz-PW-4m-compacts. HP-2 was somewhat less dense and more easily fractured.

Hot Pressing of Cement and Cement: PW-6 Mixtures - D. M. Roy and G. R. Gouda

Equipment. A 1/2-in. diameter hot pressing cell was used to prepare a series of hot pressed cement and cement: PW-6 specimens. A larger 1 in. diameter cell was designed and the materials for construction acquired.

Cement Composition. Seven common cement compositions (of which three were studied for the first time) were hot pressed under a variety of conditions. All produced dense relatively impermeable specimens, for which typical data are given in Table 11.

Cement: Waste Mixtures. PW-6 calcine was used as received from PNL (fired 1 hr at 500°C). Initial hot pressing experiments used water/solids ratio of 0.095, but because of the high volatile content of PW-6 (chiefly $NaNO_3$) later mixtures used w/s ratio = 0.03 and 0.02, and the resultant compacts have very acceptable properties. In such materials any potential effects of radiolysis of OH^- would thereby be reduced also. Data summarizing some experiments are given in Table 11.

Mechanical Properties. Compressive strengths of hot pressed cement compacts (directly from the hot press cell) range in the vicinity of 50,000 psi or higher (Table 11, Sample No. 9). Compressive strengths of Cement: PW-6 mixtures appear to be somewhat lower (Table 11, Sample No. F-1), although they are still very high strength, and very dense. One tensile strength measurement (Table 11, Sample No. C-1) was about 8 times that of normal cement.

Physical and Chemical Characteristics

- Density. Measured on a few samples, it was always higher with cement PW-6 mixtures, than with cement alone, indicating good compaction.
- Thermal stability. All cements used are quite stable in the range up to 500 - 600°C. However, Fondu cement, as expected had unusual thermal stability. When pressed at 250°C, 50,000 psi, 1/2 hr (Table 11,

TABLE 11. Hot Pressing of Cements

HOT PRESSING OF CEMENTS AND CEMENT-PW-6 MIXTURES

SAMPLE NUMBER	CEMENT COMPOSITIONS WT. % MAJOR COMPONENTS	T (°C)	P (psi)	TIME (hrs)	OTHER PARAMETERS	OBSERVATIONS
1	PORTLAND TYPE I 65 CaO, 22 SiO_2, 5.5 Al_2O_3, SO_3 = 2.6	25°	1 atm	24	w/c = 0.22	REFERENCE
2	PORTLAND TYPE I 65 CaO, 22 SiO_2, 5.5 Al_2O_3, SO_3 = 2.6	250°	50,000	1	w/c = 0.095	GOOD CYLINDER
4	PORTLAND TYPE III 63 CaO, 22 SiO_2, 5.2 Al_2O_3, SO_3 = 3.8	25°	1 atm	24	w/c = 0.22	REFERENCE; MODERATE ACID DAMAGE
5	PORTLAND TYPE III 63 CaO, 22 SiO_2, 5.2 Al_2O_3, SO_3 = 3.8	250°	50,000	1/2	w/c = 0.095	GOOD CYLINDER HIGH RESISTANCE TO ACID
8	FONDU 38 CaO, 25 SiO_2, 40 Al_2O_3, 11 Fe_2O_3	25°	1 atm	24	w/c = 0.16	REFERENCE DISINTEGRATES RAPIDLY IN ACID[a]
9	FONDU	250°	50,000	1/2	w/c = 0.095	GOOD STRONG CYLINDER DENSITY = 2.84 gm/cc σ_{COMP} = 51,400 REACTS MORE SLOWLY IN ACID THAN 8; CYLINDER REMAINS
11	SERCAR 250 26 CaO, 0.2 SiO_2, 72 Al_2O_3	25°	1 atm	24	w/c = 0.22	REFERENCE
12	SERCAR 250	250°	50,000	1/2	w/c = 0.095	GOOD CYLINDER
14	REGULATED SET 58 CaO, 16 SiO_2, 10 Al_2O_3, 6.4 SO_3	25°	1 atm	24	w/c = 0.22	REFERENCE
15	REGULATED SET 58 CaO, 16 SiO_2, 10 Al_2O_3, 6.4 SO_3	300°	50,000	1/4	w/c = 0.095	GOOD CYLINDER
16	EXPANSIVE CEMENT	25°	1 atm	24	w/c = 0.22	REFERENCE
17	EXPANSIVE CEMENT	300°	50,000	1/4	w/c = 0.095	GOOD CYLINDER
A-1	90 TYPE I CEMENT 10 PW-6	250°	50,000	1/2	w/s = 0.12	PISTONS STICK
B-1	80 TYPE I CEMENT 20 PW-6	150°	75,000	1/4	w/s = 0.04	YELLOW PPT ON PISTONS; EASILY REMOVABLE
C-1	90 TYPE I CEMENT 10 PW-6	150°	75,000	1/2	L/s = 0.07	DENSITY = 2.96 $\sigma_{TENSILE}$ = 3600 psi
F-1	80 FONDU 20 PW-6	250°	50,000	1/2	w/s = 0.03	GOOD CYLINDER; LITTLE YELLOW PPT. DENSITY = 2.97 σ_{COMP} = 33,600 psi REACTS MORE RAPIDLY THAN 9
H-1	75 FONDU 20 PW-6 5 ZEOLITE	250°	50,000	1/2	w/s = 0.03	WHITE PPT[b] CAUSES STICKING GOOD CYLINDER
I-1	80 TYPE III 20 PW-6	250°	50,000	1/2	w/s = 0.03	WHITE PPT[b] GOOD CYLINDER, LIGHT BROWN
J-1	80 WHITE CEMENT (LOW Fe) 20 PW-6	250°	50,000	1/2	w/s = 0.02	GOOD CYLINDER, LIGHT BROWN, DARK SPOTS
K-1	80 REG. SET 20 PW-6	250°	50,000	1/2	w/s = 0.02	GOOD CYLINDER, BROWN COLOR, DARK SPOTS, EASY TO REMOVE FROM CELL MORE PPT
5	100 PW-6	210°	50,000	1/2	LATEX/SOLID = 0.089	GOOD CYLINDER WHITE PPT; FOAMY YELLOW PPT OUTSIDE CELL RAPID DISINTEGRATION IN HCl

ABBREVIATIONS:

w/c = WATER:CEMENT RATIO (WT)

w/s = WATER:SOLIDS RATIO (WT)

L/s = LATEX SUSPENSION (50% SOLIDS):SOLIDS (CEMENT + WASTE)

σ_{COMP} = COMPRESSIVE STRENGTH

$\sigma_{TENSILE}$ = TENSILE STRENGTH

a = HCl 1:1 ACID

b = PPT (PRECIPITATE) = $NaNO_3$

Sample No. 9), no disintegration was observed on heating the compact to 1200°C, while Portland cement compacts underwent some fracturing.

Safety Analysis - W. K. Winegardner, T. H. Smith and G. Jansen

The purpose of the safety analysis task is to define and investigate waste management systems in relation to the containment, immobilization, and isolation of hazardous wastes and to evaluate the radiological safety implications of these systems.

Work resumed on the definition of a reference, state-of-art system for the 100-year management of high-level waste. The system, discussed previously in the April-June 1973 Quarterly report,[a] is the basis for current risk (safety) analyses. Work during the report period centered on the development of system activity levels and the definition of waste characteristics. Risk is defined as the product of the probability of postulated release incidents and the radiological consequences of these incidents.

Activity levels must be established to estimate probability, while a variety of waste characteristics is needed to evaluate consequences. Additional studies are in progress on establishing the population distribution surrounding the reprocessing plant and the Retrievable Surface Storage facility and on establishing preliminary fault trees for parts of the system.

Activity Levels

The reference system is based on projections, to the year 2000, of wastes from the U.S. Nuclear Power Industry.[b] Probabilities, and therefore risk, will be estimated from activity levels associated with the year 2000, as shown in Figure 28.

(a) W. K. Winegardner, "Safety Analysis," Quarterly Progress Report, Research and Development Activities, Waste Fixation Program, April-June 1973, BNWL-1761, July 1973.

(b) J. P. Nichols, et al., "Projections of Fuel Reprocessing Requirements and High Level Wastes from the U.S. Nuclear Power Industry," ORNL-TM-3965 (draft), to be published.

1. LIQUID STORAGE - 5 YEAR INVENTORY FROM 1996-2000 REPROCESSING (3.4×10^6 GAL)
2. LIQUID TRANSFER - 5.0×10^5 GAL PER YEAR
3. SOLIDIFICATION AND CANNING - 750 CANISTERS PER YEAR
4. CANISTER TRANSFER - 750 CANISTERS PER YEAR
5. SOLID STORAGE - 3,100 CANISTERS, 5 YEAR INVENTORY FROM 1991-1995 REPROCESSING
6. CASK LOADING - 500 CANISTERS PER YEAR
7. SHIPPING - 55 SHIPMENTS OF 10 YEAR OLD WASTE PER YEAR
8. CASK UNLOADING - 500 CANISTERS PER YEAR
9. SOLID STORAGE - 24,000 CANISTERS, 18 YEAR INVENTORY FROM 1973-1990 REPROCESSING
10. CASK LOADING - 5,000 CANISTERS PER YEAR
11. SHIPPING - 450 SHIPMENTS OF 100 YEAR OLD WASTE PER YEAR
12. MINE (BEDDED SALT) EMPLACEMENT - 5,000 CANISTERS PER YEAR

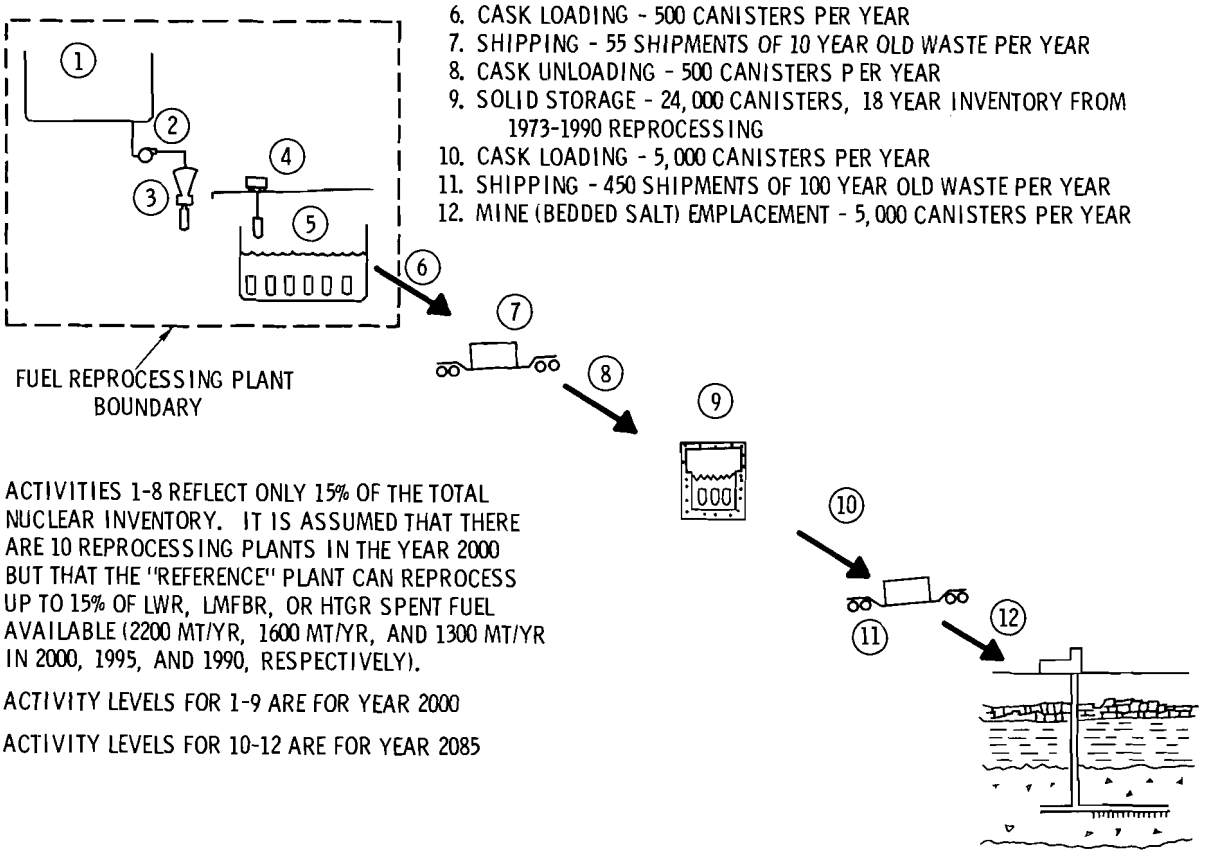

1. ACTIVITIES 1-8 REFLECT ONLY 15% OF THE TOTAL NUCLEAR INVENTORY. IT IS ASSUMED THAT THERE ARE 10 REPROCESSING PLANTS IN THE YEAR 2000 BUT THAT THE "REFERENCE" PLANT CAN REPROCESS UP TO 15% OF LWR, LMFBR, OR HTGR SPENT FUEL AVAILABLE (2200 MT/YR, 1600 MT/YR, AND 1300 MT/YR IN 2000, 1995, AND 1990, RESPECTIVELY).
2. ACTIVITY LEVELS FOR 1-9 ARE FOR YEAR 2000
3. ACTIVITY LEVELS FOR 10-12 ARE FOR YEAR 2085

FIGURE 28. 100-Year Reference Waste Management System (Activity Levels)

Waste Characteristics

Inventories. Liquid and solid inventories are based on the following values:

Reactor Type	Liquid (liters/MT)	Solid (liters/MT
LWR	378	57
HTGR	3785	170
LMFBR	1249	85

Liquid Waste Constituents. Constituents of high-level liquid wastes (other than a detailed listing of fissions products) associated with the system are summarized in Table 12.

Solid Wastes - Physical Properties. Physical properties are summarized below.

	Bulk Density g/mℓ	Thermal Conductivity $W/(m^2)(°C/m)$	Heat Capacity cal/(g)(°C)
Calcine (granular)	1.5	0.25	0.20
Glass-Ceramic	3.0	1.0	0.20

Solid Wastes - Release Properties. Values that will be used for estimating release to water are tabulated below.

	Glass-Ceramics (gm/cm^2-day)		Calcines (gm/cm^2-day)
	25°C Water	100°C Water	
Short term (day long) release	1×10^{-4}	5×10^{-3}	1.0
Long term (year long) release	5×10^{-6}	3×10^{-4}	1.0

The extent of volatile release will be estimated using the conservative curves of Figure 29. Information to aid in estimating release as the result of impact or explosion is needed.

Shipping Form. Transportation risk analyses are being based on waste in the form of a glass or ceramic, clad with austenitic stainless steel. It

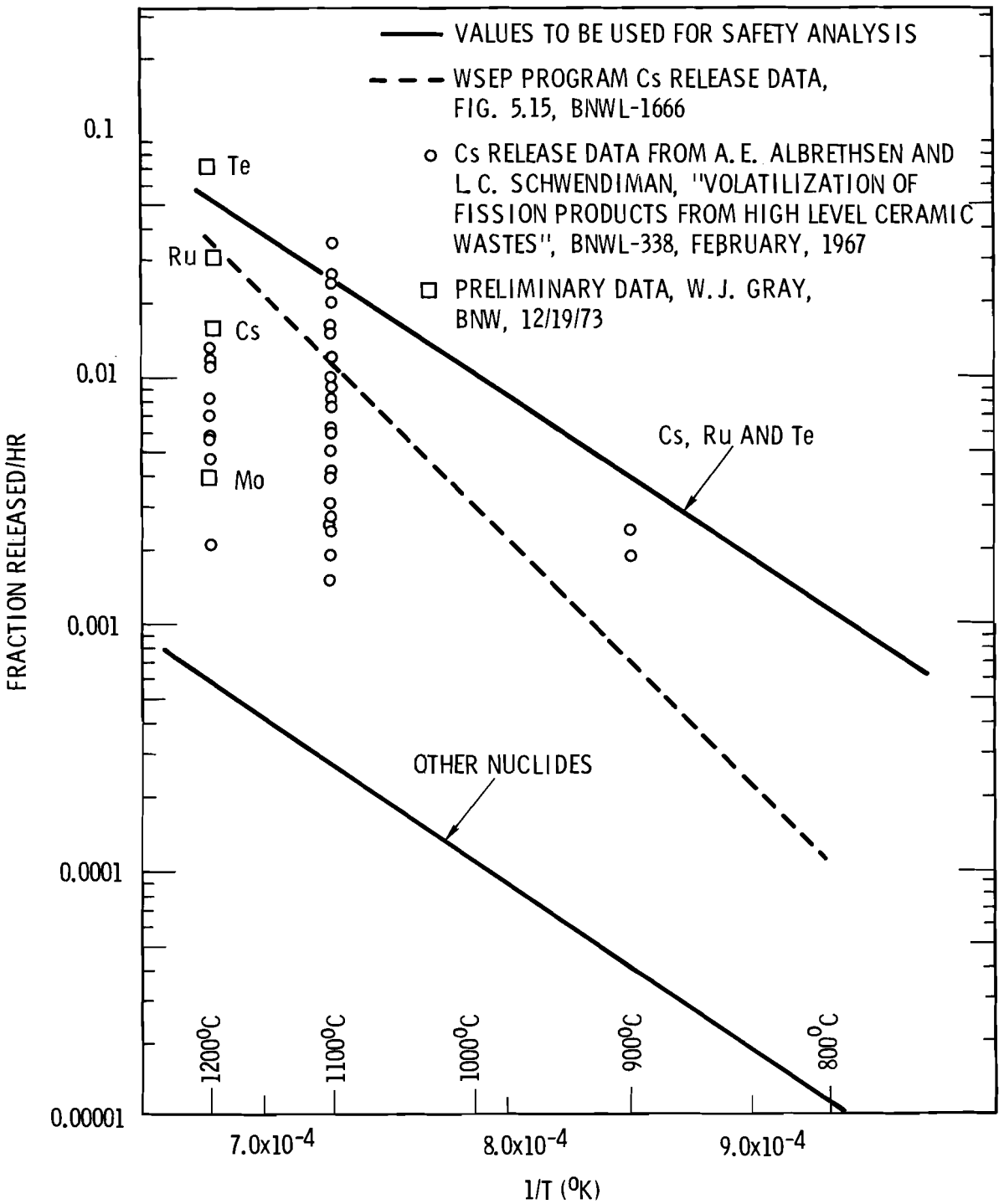

FIGURE 29. Data for Volatilization from Solidified High Level Waste

TABLE 12. Constituents of High-Level Liquid Wastes

Constituent	Grams/metric ton (MT) from Reactor Type		
	LWR[a]	HTGR[b]	LMFBR[c]
H	378	3,820	1,261
Fe	1,054	1,514	26,229
Ni	110	416	3,272
Cr	234	265	6,919
Si	-	189	-
Li	-	151	-
B	-	984	-
Mo	-	38	-
Al	-	6,359	-
Cu	-	38	-
BO_3	-	-	98,040
NO_3	65,770	435,275	243,555
PO_4	900	-	-
SO_4	-	1,060	-
F	-	1,855	-
U[d]	4,780	265	4,322
Th[d]	-	4,201	-
Pu[d]	45	1,022	475
Total Fission Products	28,800	79,409	32,961
Total Actinides	5,480	7,002	6,357

a. U-235 enriched PWR, using 378 liters of aqueous waste per metric ton, 33,000 MWd/MT exposure.
b. Combined waste from separate reprocessing of "fresh" fuel and fertile particles, using 3,785 liters of aqueous waste per metric ton, 94,200 MWd/MT exposure.
c. Mixed core and blanket, with boron as soluble poison, 10% of cladding dissolved, 1,249 liters per metric ton, 37,100 MWd/MT exposure.
d. 0.5% product loss to waste.

is assumed that the waste is shipped in 12 in. ID x 10 ft long x 0.38 in. wall canisters having welded closures. Waste volume per canister will be 6.28 ft^3 (8 ft fill). For U-enriched fuel with 33,000 MWD/MT exposure and a waste concentration of 2 ft^3/MT, canister heat generation would be 5.6 kW, 3.4 kW, and 0.4 kW after 5, 10, and 100 years, respectively.

AEC WASTE FIXATION

Ceramic Materials-Molten AEC Waste Compatibility - J. L. Bates

Ceramic refractories are being tested in a simulated molten AEC waste glass to determine their compatibility for use in an electric, ceramic-lined waste glass melter. The static test used in this study is identical to that described for the commercial waste compatibility studies described elsewhere in this report and in a previous quarterly report.[a]

The simulated molten AEC waste was composed of 70 wt% basalt and 30 wt% simulated salt cake. The simulated salt cake was made up of 67 wt% $NaNO_3$, 15 wt% $Na_2Al_2O_4$, 15 wt% Na_2CO_3, and 3 wt% NaOH. The molten mixture was heated at 1450°C in a platinum crucible in air and the refractory oxide sample was partially immersed for 48 hr.

Tests were performed for

- Fused cast SiO_2
- Fused cast ZAS (zirconium-aluminum-silicate)
- ZrO_2 castable (95% ZrO_2)
- Fused cast chrome ore (79% Cr_2O_3 from two different sources)
- SiC (glow bar)
- Sintered Zircon (ZrO_2-SiO_2)
- Isopressed chrome ore (79% Cr_2O_3)

The ZrO_2 and fused cast chrome ore (from two different suppliers) were the only refractories which did not react extensively with this waste composition.

(a) Quarterly Progress Report, BNWL-1788, pp. 7-9, October 1973.

The ZrO_2 and fused chrome ore did exhibit some small areas which did react with the molten waste glass. Other areas did not react. These variations could result from the inhomogeneity in the refractories.

The isopressed chrome ore was exposed for 120 hr to the waste glass and fractured during removal from the furnace. It was subsequently removed when the glass was cooled and broken. The reaction was greater than that for the fused cast Cr_2O_3 ore, but less than that for those samples which exhibited extensive reaction.

The silicon carbide was completely dissolved in the waste glass.

Preliminary results suggest that the corrosion of the refractories results from the reaction between the sodium in the waste glass (approximately 23 wt%) and the SiO_2 in the refractories. For example, the degree of reaction was most severe with the fused SiO_2. Lesser, but significant reaction was observed in the ZAS and Zircon. The fused cast Cr_2O_3 ore contains only small amounts of SiO_3 ($\sim$1.3 wt%) and the ZrO_2 contains less than 1% SiO_2. The resistance of SiC to oxidation is dependent upon the surface formation and oxidation resistance of SiO_2. If the glass dissolved the SiO_2, the SiC would be readily attacked by the liquid glass.

The metallographic examination of these refractories is continuing, and more extensive quantitative characterizations will be made. Those exhibiting the best resistance to attack will be heated for a longer period of time. In addition, tests will be made using another proposed waste composition containing 65 wt% basalt, 30 wt% simulated salt cake, and 5 wt% B_2O_3.

DISTRIBUTION

No. of Copies	
OFFSITE	
	UNITED STATES
1	AEC Chicago Patent Group A. A. Churm
2	AEC Directorate of Licensing for Fuels and Materials 4915 St. Elmo Ave. Bethesda, MD 20014 Deputy Director for Fuels and Materials S. H. Smiley Chief, Technical Support Branch for Fuels and Materials R. B. Chitwood
1	AEC Division of Biomedical and Environmental Research W. G. Belter
2	AEC Division of Production and Materials Management F. P. Baronowski W. L. Lennemann
2	AEC Division of Reactor Research and Development Assistant Director for Reactor Technology E. E. Sinclair Chief, Fuel Recycle Branch W. H. McVey
7	AEC Division of Waste Management and Transportation G. H. Daly W. K. Eister O. P. Gormley A. F. Perge F. K. Pittman R. W. Ramsey R. D. Walton
1	AEC Idaho Operations Office K. K. Kennedy

No. of Copies	
1	AEC Oak Ridge Operations Office E. H. Hardison
1	AEC Office of the Commissioners W. H. Beach, Technical Assistant to Commissioner C. E. Larson
1	AEC Savannah River Operations Office P. D. Fairchild
194	AEC Technical Information Center
5	Allied Chemical Corporation Idaho Falls, ID 83401 J. A. Buckham B. R. Dickey D. W. Rhodes C. M. Slansky B. R. Wheeler
3	Allied-Gulf Nuclear Services P. O. Box 847 Barnwell, SC 29812 B. M. Legler G. R. Bray A. Schneider
1	Argonne National Laboratory R. C. Vogel
1	Bechtel Corporation 50 Beale Street San Francisco, CA 94119
1	Burns and Roe, Inc. 700 Kinderamack Road Oradell, NJ 07649 P. P. DeRienzo
1	C-E Refractories Box 828 Valley Forge, PA 19482 Alfred W. Allen

No. of Copies	
1	Corning Glass Works Technical Staffs Division Corning, New York 14830 M. G. Britton
2	Dow Chemical Company (AEC) D. L. Ziegler M. A. Thompson
4	duPont Company, Aiken (AEC) C. H. Ice A. S. Jennings L. H. Meyer R. W. Wallace
1	duPont Company, Wilmington (AEC) A. A. Johnson
2	Environmental Protection Agency Parklawn Building 5600 Fishers Lane Rockville, MD 20852 C. G. Meyers
1	Environmental Protection Agency P. O. Box 15027 Las Vegas, NV 89114 B. Mann
1	Environmental Protection Agency 5555 Ridge Avenue Cincinnati, OH 45213 R. E. Landreth
1	General Electric Company 175 Curtner Avenue (M/C 160) San Jose, CA 95125 R. G. Barnes
1	General Electric Company Midwest Fuel Recovery Plant Route 1, Box 219-B Morris, IL 60450 R. Lambert

No. of Copies	
2	General Electric Company Vallecitos Nuclear Center Vallecitos Road Pleasanton, CA 94566 W. H. Reas
3	Gulf Energy and Environmental Systems P.O. Box 81608 San Diego, CA 92138 L. H. Brooks J. J. Shefcik M. E. Spaeth
1	Los Alamos Scientific Laboratory (AEC) C. W. Christenson
1	National Lead Company 111 Broadway New York, NY 10006 Stephen Brown
1	National Academy of Sciences Committee of Radioactive Waste Management National Research Council 2101 Constitution Avenue Washington, DC 20418 D. Cyrus Klingsberg, Tech. Secretary
2	Nuclear Fuel Services, Inc. P.O. Box 124 West Valley, NY 14171 J. P. Duckworth, Plant Manager 6000 Executive Blvd., Suite 600 Rockville, MD 20852 E. D. North, Director of Technical Administration
1	NYS Atomic and Space Development Authority 230 Park Ave., Rm. 2425 New York, NY 10017 J. G. Cline, General Manager

No. of Copies	
4	Oak Ridge National Laboratory (AEC) Central Research Library, Document Reference Section Central Research Library, ORNL Laboratory Records Dept., ORNL Laboratory Records Dept., ORNL-RC
1	Penberthy Electromelt 631 S. 96th Street Seattle, WA 98108 L. Penberthy
1	Pennyslvania State University Materials Research Laboratory University Park, PA 16802 G. J. McCarthy
2	Sandia Laboratories Albuquerque, NM 87107 A. C. Zuppero R. L. Hagengruber
4	Union Carbide Corporation (ORNL) A. L. Boch J. O. Blomeke F. Gera H. W. Godbee
	FOREIGN
1	Atomic Energy of Canada Ltd. Pinawa, Manitoba, ROE 1LO CANADA P. J. Dyne
1	Atomic Energy of Canada Ltd. Chalk River, Ontario CANADA J. A. Morrison
1	Atomic Energy of Canada Ltd. Sheridan Park, Ontario CANADA W. M. Campbell

No. of Copies	
1	EURATOM Health Physics Division 29, Rue Aldringer Luxembourg, BELGIUM Rene Amavis
1	Studiecentrum voor Kernenergie (Mol) SCK, CEN Boeretang, 200 2400 Mol. BELGIUM P. Dejonghe
1	Atomic Energy Research Establishment Harwell, Didcot, Berks, ENGLAND K. D. B. Johnson
1	United Kingdom Atomic Energy Authority Risley, ENGLAND D. W. Clelland
2	Centre de Marcoule B. P. 106 30 - Bagnols S/Ceze FRANCE R. Bonniaud
3	Centre d'Etudes Nucleaires de Fontenay-aux-Roses Boite Postale 6 92 - Fontenay-aux-Roses FRANCE P. J. Regnaut J. Sauteron Y. J. Sousselier
1	Bundesministerium für Bildung und Wessenschaft D53 Bonn 12 Postfach 120124 GERMANY R. P. Randl

No. of Copies	
1	Gesellschaft für Strahlen und Umwellforschung Institut für Tieflogerung 3392 Clausthal -Zellerfeld Bornhardstr. 22 GERMANY K. Kühn
1	Hahn-Meitner-Institut 1 Berlin 39 Glienickerstr. 100 GERMANY Hans W. Levi
2	Institut für Chemische Technologie Kernforschungsanloge Julich GmbH D517 Julich Postfach 365 GERMANY E. R. Merz K. H. Rattay
1	MGH/GWK/Wiederacifurbeitung - Sanlage/WAK Karlsruhe, GERMANY W. A. Issel
2	Nuclear Research Center Waste Management Dept. D75 Karlsruhe Weberstr. 5 GERMANY H. Krause
2	CNEN Directtore of Programma Eurex Del CNEN Saluggia "Vercelli", ITALY Giacomo Calleri Laboratorio di Ingegneria Sanitaria Via Anguillarese km 1 + 300 Roma, ITALY Willy Bocola

No. of Copies	
1	Bhabha Atomic Research Centre Organic Waste Laboratory Plutonium Plant Site Trombay, Bombay, INDIA Keshava Chandra
2	Bhabha Atomic Research Centre Waste Treatment Division Trombay, Bombay, INDIA N. S. Sunder Rajan K. T. Thomas
1	India Atomic Energy Establishment Waste Treatment Plant & Decontamination Center Bombay 85, INDIA Victor Amalraj, Plant Superintendent
2	International Atomic Energy Agency Kartner Ring 11 P.O. Box 590 A-1011, Vienna, AUSTRIA
1	Dr. H. F. Ramdohr c/o Friedrich Uhde GmbH 46 Durtmund Deggingstr. 10-12 GERMANY

ONSITE

1	AEC/RL Patent Attorney R. W. Poteat
3	AEC Richland Operations Office Production and Waste Management Programs Division O. J. Elgert (2) Research and Development Programs Division B. J. Melton
1	AEC/RL Environmental, Safety and Technical Services Division P. G. Holsted

No. of Copies	
12	Atlantic Richfield Hanford Company

L. E. Brownell
M. H. Campbell
R. E. Isaacson
H. P. Shaw
W. W. Shultz/M. J. Kupfer
A. E. Smith
P. W. Smith
M. J. Szulinski
J. H. Warren
D. D. Wodrich
File Copy

2 Exxon
Richland, WA 99352

S. J. Beard
L. T. Lakey

2 United Nuclear Industries, Inc.

2 Westinghouse Hanford Company

G. L. Richardson
C. R. Cooley

34 Battelle-Northwest

E. L. Alpen
R. J. Bashor
J. L. Bates
W. F. Bonner
N. E. Carter
T. D. Chikalla
D. L. Condotta
G. M. Dalen
R. D. Dierks
J. N. Hartley
G. Jansen
J. D. Kaser
J. L. McElroy (5)
J. E. Mendel
D. F. Newman
A. M. Platt
E. Porath
A. K. Postma
J. Posakoni
W. A. Ross
K. J. Schneider
D. H. Siemens
W. H. Swift
W. K. Winegardner
Technical Information (5)
Technical Publications